Proteomic Studies of a Single CNS Synapse Type: The Parallel Fiber/Purkinje Cell Synapse

Fekrije Selimi[1,2,3], Ileana M. Cristea[4,5], Elizabeth Heller[1], Brian T. Chait[4], Nathaniel Heintz[1*]

1 Laboratory of Molecular Biology, Howard Hughes Medical Institute, The Rockefeller University, New York, New York, United States of America, **2** CNRS, UMR7102, Paris, France, **3** UPMC, UMR7102, Paris, France, **4** Laboratory for Mass Spectrometry and Gaseous Ion Chemistry, The Rockefeller University, New York, New York, United States of America, **5** Department of Molecular Biology, Princeton University, Princeton, New Jersey, United States of America

Precise neuronal networks underlie normal brain function and require distinct classes of synaptic connections. Although it has been shown that certain individual proteins can localize to different classes of synapses, the biochemical composition of specific synapse types is not known. Here, we have used a combination of genetically engineered mice, affinity purification, and mass spectrometry to profile proteins at parallel fiber/Purkinje cell synapses. We identify approximately 60 candidate postsynaptic proteins that can be classified into 11 functional categories. Proteins involved in phospholipid metabolism and signaling, such as the protein kinase MRCKγ, are major unrecognized components of this synapse type. We demonstrate that MRCKγ can modulate maturation of dendritic spines in cultured cortical neurons, and that it is localized specifically to parallel fiber/Purkinje cell synapses in vivo. Our data identify a novel synapse-specific signaling pathway, and provide an approach for detailed investigations of the biochemical complexity of central nervous system synapse types.

Citation: Selimi F, Cristea IM, Heller E, Chait BT, Heintz N (2009) Proteomic studies of a single CNS synapse type: The parallel fiber/Purkinje cell synapse. PLoS Biol 7(4): e1000083. doi:10.1371/journal.pbio.1000083

Introduction

Each of the thousands of cell types present in the nervous system receives multiple classes of inputs that are spatially segregated and functionally distinct. The chemoaffinity hypothesis stated that "the establishment and maintenance of synaptic associations were conceived to be regulated by highly specific cytochemical affinities…." [1]. Support for this idea has come from studies of specific synaptic proteins [2,3]. For example, different sets of neurotransmitter receptors are found at different synapse types [3], even at excitatory synapses made on the same neuron [4]. Precise subcellular targeting of synapses is also dependent on the recognition of specific molecules such as adhesion proteins [5]. In addition to these direct-recognition mechanisms, guidepost cells seem to target synapse formation to precise locations: their role has been demonstrated in both invertebrates [6] and vertebrates [7]. Synaptic physiology is also regulated by mechanisms that are synapse type-dependent, since similar stimulation patterns can have opposite effects on plasticity of different synapses [8]. Therefore, the formation and function of each type of synapse is controlled by a complex activation of signaling pathways through specific proteins.

Since the visualization of synapses by electron microscopy, attempts have been made at biochemically purifying them and at identifying their chemical composition, especially for the postsynaptic densities characteristic of excitatory synapses [9,10]. The use of mass spectrometry (MS) to identify proteins in complex mixtures has greatly improved our ability to unravel the protein composition of organelles. Using this technique, over 1,000 different postsynaptic proteins have been identified in "bulk" postsynaptic density preparations or in affinity-purified receptor complexes [11–16]. These proteins have a wide range of functions: receptors to neurotransmitters, scaffold proteins, kinases, enzymes, etc. Recently, combining comparative genomics and proteomics, Emes and collaborators [17] have shown that increased behavioral complexity correlates with a phylogenetic expansion of synaptic proteins that are involved in upstream signaling pathways, such as receptors and adhesion molecules. Microarray analysis also showed a very variable regional expression pattern for these upstream synaptic proteins [17], in accordance with previously obtained results for neurotransmitter receptors [3]. The complexity of the synaptic proteome illustrated by these data highlights the need for studies aimed at systematically identifying the protein composition of individual synapse types, and understanding their mechanistic diversity.

To address this issue, we have developed synaptic protein profiling as an approach to isolate and biochemically characterize specific types of central nervous system (CNS) synapses. We chose to analyze first the parallel fiber to

Academic Editor: Huda Y. Zoghbi, Baylor College of Medicine, United States of America

Received November 14, 2008; **Accepted** March 2, 2009; **Published** April 14, 2009

Abbreviations: BAC, bacterial artificial chromosome; CID, collision-induced dissociation; CNS, central nervous system; eGFP, enhanced green fluorescent protein; GFP, green fluorescent protein; MALDI, matrix-assisted laser desorption/ionization; MALDI-IT, matrix-assisted laser desorption/ionization ion trap; MS, mass spectrometry; MS/MS, tandem mass spectrometry; PF/PC synapse, parallel fiber to Purkinje cell synapse; PSD, postsynaptic density; QqTOF, quadrupole/time-of-flight

* To whom correspondence should be addressed. E-mail: heintz@mail.rockefeller.edu

Author Summary

The brain is composed of many different types of neurons that form very specific connections: synapses are formed with specific cellular partners and on precise subcellular domains. It has been proposed that different combinations of molecules encode the specificity of neuronal connections, implying the existence of a "molecular synaptic code." To test this hypothesis, we describe a new experimental strategy that allows systematic identification of the protein composition for individual synapse types. We start with mice that are genetically engineered to facilitate the purification of one type of synapse from a given neuronal population in the central nervous system, the parallel fiber/Purkinje cell synapse. The purification is performed using a combination of biochemical fractionation and affinity purification. Subsequent mass spectrometry allows us to identify approximately 60 different proteins present in the resulting sample. We have further analyzed some of the 60 proteins and show that MRCKγ, a newly identified kinase, is localized in the dendritic spines where the parallel fiber/Purkinje cell synapses are formed and that it can modulate the morphogenesis of dendritic spines. The use of this experimental strategy opens up the ability to provide insights into the underlying "molecular code" for the diverse types of synapses in the brain.

Purkinje cell (PF/PC) synapse in the cerebellum, because of its unique physiological properties and its involvement in neurological disease [18,19]. We engineered mice to tag and purify specifically PF/PC synapses and, using MS, we have identified 65 proteins located at the PF/PC synapse. This dataset provides clues to PF/PC synapse-specific signaling pathways, as illustrated by our functional analysis of one of these proteins, MRCKγ. Our results provide an important example of the biochemical complexity of an individual synapse type, and reveal a new mechanism for the regulation of synaptic function.

Results

Purifying the Parallel Fiber/Purkinje Cell Synapse

To enable purification of PF/PC synapses, we developed a transgenic line that expresses an affinity tag only at the PF/PC synapse. We generated a fusion between the glutamate receptor delta2, GluRδ2 (National Center for Biotechnology Information [NCBI]# EDK98768), which is specifically localized at the PF/PC postsynaptic density [20], and Venus, a variant of the green fluorescent protein (GFP). The resulting fusion protein, VGluRδ2, is properly processed and transported to the cell surface (Figure S1). To express the fusion specifically in cerebellar Purkinje cells, the VGluRδ2 cDNA was then incorporated into a Pcp2 bacterial artificial chromosome (BAC) by homologous recombination, and the resulting Pcp2/VGluRδ2 BAC construct was used to generate transgenic mice (Figures 1A and S1). Expression of the fusion polypeptide was detected in the cerebellar extracts of Pcp2/VGluRδ2 transgenic mice (Figure 1B), and coimmunoprecipitation experiments demonstrated proper assembly of the VGluRδ2 fusion with the endogenous GluRδ2 receptor subunits (Figure 1C). As shown in Figure 1D, the localization of VGluRδ2 in the molecular layer and somata of PCs agrees with the synaptic localization of the GluRδ2 receptor. In contrast, the enhanced GFP (eGFP) control protein expressed using the same BAC vector (Pcp2/eGFP; http://www.gensat.org) is detected throughout the cell, including marked labeling of both Purkinje cell dendrites and axons (Figure 1D). Prior to the affinity-purification step, we sought to produce cerebellar extracts enriched for synaptic structures relative to trafficking complexes, and to maximize the recovery of VGluRδ2-tagged postsynaptic densities (PSDs). This was performed by fractionation of a solubilized crude synaptosome fraction (S3) on a gel-filtration column (Figure 2A). As shown in Figure 2B and 2C, this resulted in an enrichment of postsynaptic and mitochondrial proteins, and a relative depletion of endoplasmic reticulum (ER) components and presynaptic proteins in the high molecular weight fractions. These excitatory synaptic fractions contain essentially all of the PSD95 scaffolding protein. They also contain VGluRδ2, which was distributed amongst the different fractions in the same manner as wild-type GluRδ2 (Figure 2C). This was also observed using a standard synaptosome purification (Figure S2) and shows that the fusion receptor VGluRδ2 is targeted to the synapse similarly to the wild-type GluRδ2.

To separate PF/PC PSDs from other cerebellar synapses, we performed affinity purification from the pooled excitatory synaptic fractions (red rectangle, Figure 2C) using an anti-eGFP antibody. Electron microscopy of the affinity purified material showed electron-dense structures that were reminiscent of PSDs [21] on the surface of the beads used for purification of VGluRδ2 extracts (Figures 3C and S3). These structures were absent from beads used to immunopurify extracts from Pcp2/eGFP control cerebella.

Using western blots, we could show that more than 50% of the target protein was immunopurified from the input extract for either the control eGFP or the VGluRδ2 extracts (Figure 3A and unpublished data). Western blotting also demonstrated copurification of several PF/PC synaptic components with VGluRδ2, including the GluRδ2 and GluR2/3 receptors, and the scaffolding proteins PSD93 and Homer (Figure 3B). Markers of inhibitory synapses (GABA(A) receptor α6, GABA(A) receptor β, and gephyrin), presynaptic structures (synapsin I and synaptophysin), or of mitochondria (Cox) did not copurify, demonstrating the specificity of this approach (Figure 3B). As expected, none of these markers copurified with soluble eGFP in extracts prepared from Pcp2/eGFP control mice (Figure 3B). Taken together, these results demonstrate that the combination of cell-specific genetic targeting, molecular tagging of specific CNS synapses, biochemical fractionation, and affinity purification can be used to enrich for a specific type of PSD from crude brain extracts.

Sixty-Five Proteins Identified in Purified Parallel Fiber/Purkinje Cell Postsynaptic Densities

To systematically identify components of the PF/PC PSDs, we analyzed the protein content of pooled PF/PC PSD preparations using single- and two-stage MS [22]. A first sample, prepared by pooling three experiments using ten Pcp2/VGluRδ2 cerebella each, enabled us to identify 12 components present at the PF/PC synapse but not present in the control sample prepared in parallel from Pcp2/eGFP cerebella (Table S1). To increase the number of PF/PC PSD components identified, we performed a second analysis on a sample prepared with a total of 50 cerebella (Figure 3D). A total of 65 proteins were identified: 37 proteins were detected with high confidence (Figures S4 and S5; Tables S1 and S3),

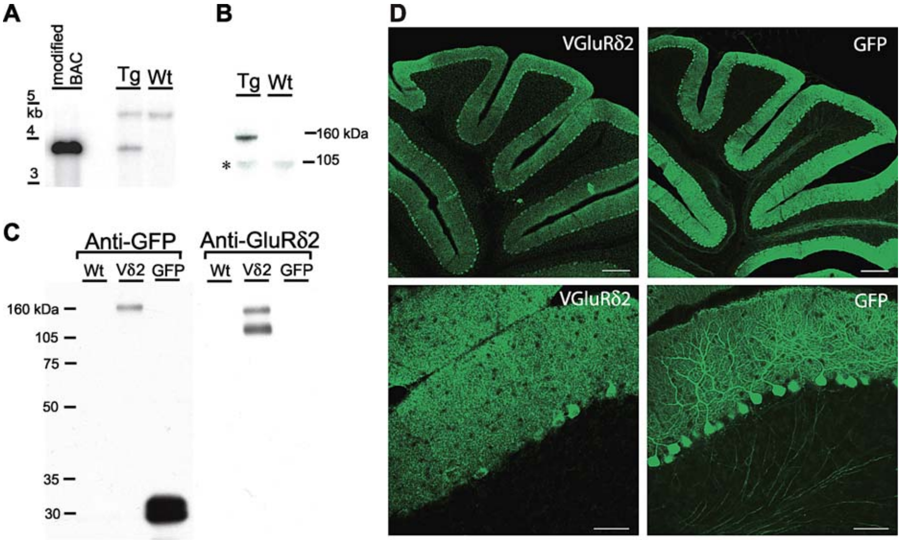

Figure 1. Tagging the Parallel Fiber/Purkinje Cell Synapse in Transgenic Mice

(A) Southern blot was used to identify transgenic mice having integrated the Pcp2 BAC (a Purkinje cell–specific driver) containing the Venus-tagged GluRδ2 receptor, VGluRδ2. Tg, transgenic; Wt, wild type.

(B) VGluRδ2 expression was detected using an anti-GFP antibody on immunoblots from total protein extracts of transgenic (Tg) versus wild-type (Wt) cerebella. An asterisk (*) indicates a nonspecific band.

(C) Both VGluRδ2 and GFP were affinity purified using an anti-GFP antibody from 1% Triton X-100 cerebellar extracts from wild-type (Wt), Pcp2/VGluRδ2 (Vδ2), and Pcp2/eGFP control (GFP) mice, as shown by probing the immunoblots with an anti-GFP antibody (left). VGluRδ2 specifically copurified the endogenous GluRδ2, as shown by probing the same blot with an anti-GluRδ2 antibody (right).

(D) Immunofluorescence on cerebellar sections using an anti-GFP antibody shows the specific localization of VGluRδ2 in the molecular layer and somata of Purkinje cells of Pcp2/VGluRδ2 mice. Soluble GFP is detected in the molecular layer, dendrites, somata, and axons of Purkinje cells in sections from Pcp2/eGFP mice. Scale bars in the upper panels indicate 200 μm; lower panels, 50 μm.

doi:10.1371/journal.pbio.1000083.g001

and 28 were observed at lower levels and identified with less confidence (Figure S6; Tables S2 and S4). This analysis confirmed the presence of the PF/PC synapse proteins GluRδ2 [23], Homer-3 [24], PSD93 [23], delphilin [23], Shank1, and Shank2 [25], and the absence of proteins located at other excitatory (NMDA receptor subunits, GABA(A) receptor α6) or inhibitory synapses (GABA(A) receptor α6, GABA(A) receptor β, and gephyrin) in the cerebellum. Forty of the identified proteins in our affinity-purified PSDs have been previously detected in preparations of synaptic proteins ([16] and Tables S1 and S2).

The 65 proteins we have identified can be grouped into 11 different functional categories (Figure 3E; Tables S1 and S2). These categories have been previously annotated in studies of the postsynaptic density [13], with the exception of a class of proteins that we have called "phospholipid metabolism and signaling." In the "scaffolds and adaptors" category, several members of the Shank family (1 and 2) and the PSD family (PSD93 and PSD95) were detected at the PF/PC synapse, illustrating redundancy for scaffold proteins, certainly due to their importance for synaptic function. Other functional categories include proteins important for synapse formation and physiology, such as regulators of small GTPases and protein kinases. Interestingly, eight of the proteins identified in our study can regulate or be regulated by phospholipid metabolism (Iptr1, synaptojanin 1 and 2, phospholipase B, ABCA12, and MRCKγ), or contain phospholipid-binding domains (Plekha7, annexin A6, and MRCKγ), and were thus grouped into a previously unrecognized category "phospholipid metabolism and signaling." This suggests that phospholipid regulation is a major feature of the PF/PC synapse. Another important category present at synapses groups receptors and ion channels: several glutamate receptor subunits and several G protein–coupled receptors (GABA-B and BAI receptors) were detected in our analysis of the PF/PC PSD. Interestingly, the extracellular domain of BAI receptors contains thrombospondin repeats, which can mediate cell adhesion [26]. Several other proteins identified at the PF/PC synapse in our study are involved in cell adhesion and interaction with the extracellular matrix: receptor protein tyrosine phosphatases [27], delta-catenin-2 [28], Neph1 [29] and laminins [30]. These diverse potential recognition proteins could form together a "code" defining the PF/PC synapse.

To provide additional evidence for the synaptic localization of the novel components that we have identified, we performed immunofluorescence studies on cerebellar sections from wild-type mice. Localization in the molecular layer of the cerebellum, which contains the PF/PC synapses, was evident for MRCKγ, Gm941, BAIAP2, RPTPm, Neph1, and delta2-catenin (Figure 4). Delta2-catenin and Gm941 could also be detected in some cerebellar interneurons. We also examined the expression of candidates reported in in situ hybridization databases (http://www.stjudebgem.org; http://www.brain-map.org; and http://www.genepaint.org). Interpretable data were available for 42 candidates, and all but two were expressed in Purkinje cells, with a majority showing little detectable expression in the granule cell layer (Tables S1 and S2). These expression data provide additional confirmation that the majority of the proteins identified in our study are bona fide components of the PF/PC synapse.

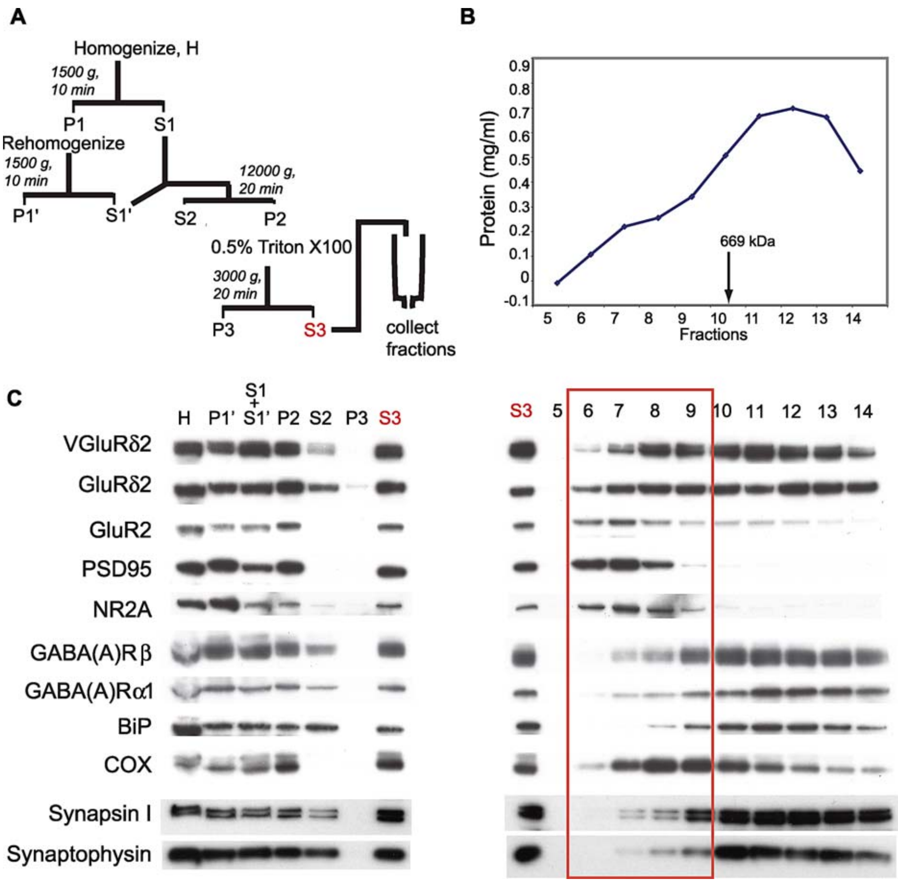

Figure 2. VGluRδ2 Is Detected in Excitatory Synaptic Fractions Using a New Purification Method

(A) We prepared a crude synaptosome P2 fraction that was solubilized in 0.5% Triton X-100 final concentration. The extract was then separated on a Sephacryl S1000 gel filtration column. Calibration of the column indicated that protein complexes smaller than 669 kDa (arrow in [B]) were resolved after fraction 10.

(B) Protein dosage was performed on every fraction collected.

(C) Each fraction (0.1% in volume) was run on western blots and assayed for the presence of excitatory postsynaptic markers (GluRδ2, GLUR2, PSD95, and NR2A), presynaptic markers (synapsin I and synaptotagmin), inhibitory synapse markers (GABA(A)Rβ and GABA(A)Rα1), the endoplasmic reticulum marker BiP, and the mitochondrial marker COX. VGluRδ2 was detected using an anti-GFP antibody. The red rectangle outlines the "excitatory synaptic" fractions enriched for synaptic markers and pooled for subsequent affinity-purification of PF/PC PSDs.

doi:10.1371/journal.pbio.1000083.g002

MRCKγ: An Example of a New Signaling Pathway at the Parallel Fiber/Purkinje Cell Synapse

Within our "phospholipid metabolism and signaling" category, we identified the kinase MRCK gamma (MRCKγ, NCBI# Q80UW5), which has not previously been localized to synapses. Since MRCK family members have been shown to regulate cytoskeleton reorganization and cell morphology [31,32], we sought to test the role of MRCKγ in dendritic spine morphogenesis in primary cortical cultures. Comparative analysis of dendritic protrusions was carried out for cultures transfected either with GFP alone, or in combination with full-length MRCKγ (MRCKγFL) or a MRCKγ construct lacking the kinase domain (MRCKγDN) (Figure 5A). Protrusion density is not significantly affected by overexpression of either form of the kinase (GFP: 9.5 ± 0.7 protrusions per 20 μm; MRCKgDN: 8.0 ± 0.6; MRCKgFL: 9.1 ± 0.6; one-way ANOVA, $p = 0.29$). However, the mean length of dendritic protrusions in neurons overexpressing MRCKγFL decreased when compared to control neurons, whereas the length of protrusions in MRCKγDN-transfected neurons increased (GFP: 1.79 ± 0.07 μm; MRCKgDN: 2.11 ± 0.08; MRCKgFL: 1.48 ± 0.06; $p < 0.05$ for all comparisons, Dunn multiple comparison test). The effect of MRCKγDN implies that it can interfere with endogenously expressed MRCK kinases. Indeed, after data mining of previously published results, we found that MRCKβ has been identified in "bulk" PSD preparations from mouse brain, and thus could be present in cortical neurons [16]. Since mean spine length decreases with maturation [33], our data demonstrate that MRCK family members, through their kinase function, increase maturation of dendritic spines in primary CNS neurons.

Given the presence of MRCKγ in our PSD preparations, and its ability to modulate dendritic spine morphogenesis, we were next interested in its subcellular localization in Purkinje cells (Figure 5B). High-resolution confocal immunofluorescence using an antibody against MRCKγ clearly demonstrated its presence in Purkinje cell dendritic spines, which have been shown to contain GluRδ2 [4]. Moreover, colabeling with markers of specific synapses on Purkinje cells showed that MRCKγ is extensively colocalized with VGluT1, a marker for

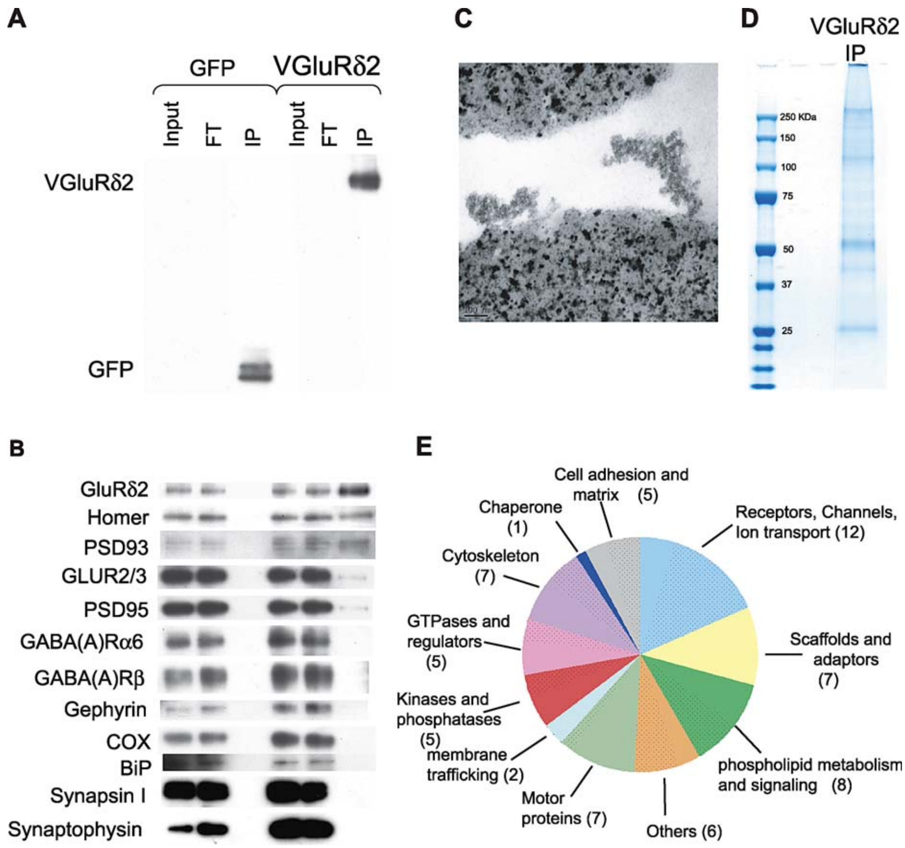

Figure 3. Affinity Purification and Protein Profiling of the Parallel Fiber/Purkinje Cell PSDs

(A) Synaptic fractions from Pcp2/VGluRδ2 animals were affinity purified using magnetic beads coated with anti-GFP antibody (VGluRδ2). In parallel, control purifications were performed on preparations from Pcp2/eGFP transgenic mice (GFP); 0.025% of the inputs and flow-throughs (FT), and 25% of the affinity-purified samples (IP) were assayed by western blot using an anti-GFP antibody and showed immunoprecipitation of both VGluRδ2 and GFP, respectively.

(B) The same blot was probed for different postsynaptic markers, presynaptic markers (synapsin I and synaptotagmin), the mitochondrial protein COX, and the ER marker BiP, showing specific copurification of postsynaptic markers localized to the PF/PC synapse.

(C) Electron microscopy shows the presence of electron-dense structures reminiscent of PSDs on the surface of the magnetic beads used for affinity purification of Pcp2/VGluRδ2 extracts.

(D) Proteins from the affinity-purified VGluRδ2 PSDs were separated by SDS-PAGE electrophoresis and stained with Coomassie Blue before MS analysis.

(E) MS identified 65 different proteins in the complexes purified from Pcp2/VGluRδ2 mice. These proteins can be classified into 11 functional categories. The number of proteins from each category is indicated in parentheses. Nonshaded areas represent proteins found with high confidence.

doi:10.1371/journal.pbio.1000083.g003

PF/PC synapses. MRCKγ is not present in structures labeled by VGluT2 or GAD65/67, which are present at climbing fiber and inhibitory Purkinje cell synapses, respectively. Taken together, our data support a specific role for MRCKγ in the maturation and plasticity of PF/PC synapses, and confirm the importance of synapse-specific protein profiling for the discovery of signaling pathways that modulate the development and function of specific CNS synapse types.

Discussion

We have demonstrated that the biochemical components of a specific synapse type from a particular neuronal population can be identified using a combination of genetically engineered mice, affinity purification, and MS. Using our approach, we have prepared a fraction enriched in PF/PC PSDs and identified 65 proteins classified in 11 different functional categories. This dataset provides information on signaling pathways specifically tethered to this synapse, as exemplified by our functional analysis of MRCKγ. It also provides information on the variety of proteins that can be part of the code defining the PF/PC synapse.

Approximately 700 different proteins have been identified in PSD preparations from whole brain [16]. However, it has been estimated that, given the mass of a single PSD, the copy number of scaffold proteins in a PSD, and an average size of 100 kDa for each synaptic protein, only about 100 different proteins can be expected to be found at one particular type of PSD [34]. The number of proteins we find in our study is consistent with that estimate. Although our analysis may not have revealed all PF/PC postsynaptic proteins, the successful identification of AMPA receptor subunits in our preparations suggests that any proteins not detected in our sample must be present at low stochiometries in the PSD.

Synaptic protein profiling can reveal novel sets of proteins that allow formulation of specific hypotheses regarding synaptic function. For example, we discovered MRCKγ at PF/PC synapses: this kinase is part of a family that has never been described at synapses. This result was striking since MRCK proteins can respond to small GTPases signaling and

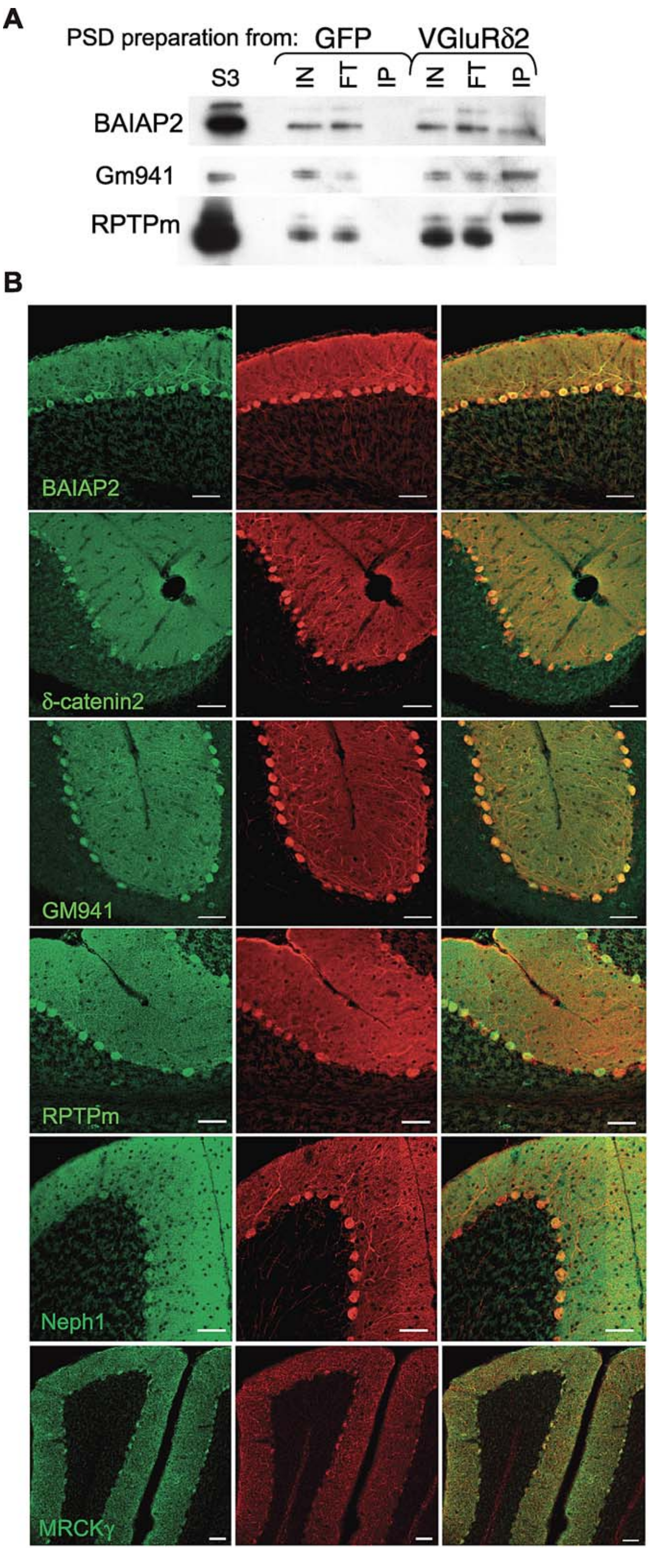

Figure 4. Localization of Several Candidate Synaptic Proteins at the Parallel Fiber/Purkinje Cell Synapses

(A) Presence of selected candidates in PF/PC PSDs purified from Pcp2/VGluRδ2 cerebella; 0.025% of the inputs (IN) and flow-throughs (FT), and 25% of the affinity-purified samples (IP) obtained from Pcp2/eGFP control (GFP) and Pcp2/ VGluRδ2 (VGluRδ2) cerebella were assayed by western blot.

(B) Localization by immunofluorescence of candidate synaptic proteins. Labeling was performed using antibodies recognizing several candidate proteins identified by MS (green) in conjunction with an anti-calbindin antibody specifically labeling Purkinje cells (red). Scale bars indicate 50 μm.

doi:10.1371/journal.pbio.1000083.g004

have been shown to modulate actin cytoskeleton and cell morphology in nonneuronal systems [31]. These characteristics immediately suggest a role for these kinases in spine morphogenesis, which we have now shown for MRCKγ using transfection of cultured cortical neurons. Taken together, these data also have implications for the study of neurodevelopmental diseases. Deficiencies in spine length and spine morphology in Purkinje cells have been found in models of mental retardation and Angelman syndrome [35,36]. Given the link between another small GTPase-dependent kinase, PAK3, and mental retardation [37], our results suggest that MRCKγ could participate in the signaling pathways involved in mental retardation and autism spectrum disorders.

Another interesting finding of our study is the presence of a high proportion of proteins involved in phospholipid metabolism and signaling at the PF/PC PSD. A major regulator of the physiology of the PF/PC synapse is the metabotropic glutamate receptor 1 (mGluR1) which induces phosphatidylinositol-4,5-P2 (PIP2) hydrolysis through activation of phospholipase C [8,18]. Our results show the presence of MRCKγ and Itpr1 in affinity-purified PF/PC PSDs: these proteins can respond to, respectively, DAG and IP3, which are the metabolites of PIP2 hydrolysis. This further supports the importance of mGluR1 signaling at the PF/PC synapse and extends the number of regulatory pathways potentially activated by mGluR1. Also included in the "phospholipid signaling and metabolism" category in our data are synaptojanin-1 and −2, two PIP2-metabolizing enzymes. These enzymes are best known for their regulation of vesicle recycling at synapses, but have also been found by other biochemical studies at PSDs [16]. Phospholipid metabolism is known to be critical for the function of the presynaptic side of the synapse, especially vesicle recycling [38]. It also plays a role in defining the boundaries of the apical pole and the localization of tight junctions in epithelial cells [39]. Our results suggest that phospholipid signaling also participates in regulating the structure and stability of PSDs. Given the fact that lithium is used as a treatment for schizophrenia and bipolar disorders, and that it might act by modulating phospholipids' metabolism [40], our results may be particularly relevant for studies of a variety of human neurological disorders. Indeed, it has been suggested that synaptojanin-1 is involved in the cognitive defects observed in Down syndrome [41], and that PIP2 metabolism may be linked to synaptic dysfunctions in Alzheimer disease [42].

The results presented here provide clues to the nature of the "synaptic code" and the types of molecules that may be critical in definition of specific synapse types. As expected from previous studies [2], we find proteins with classical adhesion domains such as Neph1 and the receptor tyrosine phosphatase RPTPmu. SYG1, the *Caenorhabditis elegans* homolog of Neph1, has been shown to define synapse location in vivo [6], and may play a similar role for the PF/PC synapse. Receptor tyrosine phosphatases play important roles in axon guidance, and have also been shown to control synapse formation [43]. We also find proteins at the PF/PC synapse with as yet unknown functions in synaptogenesis, such as the

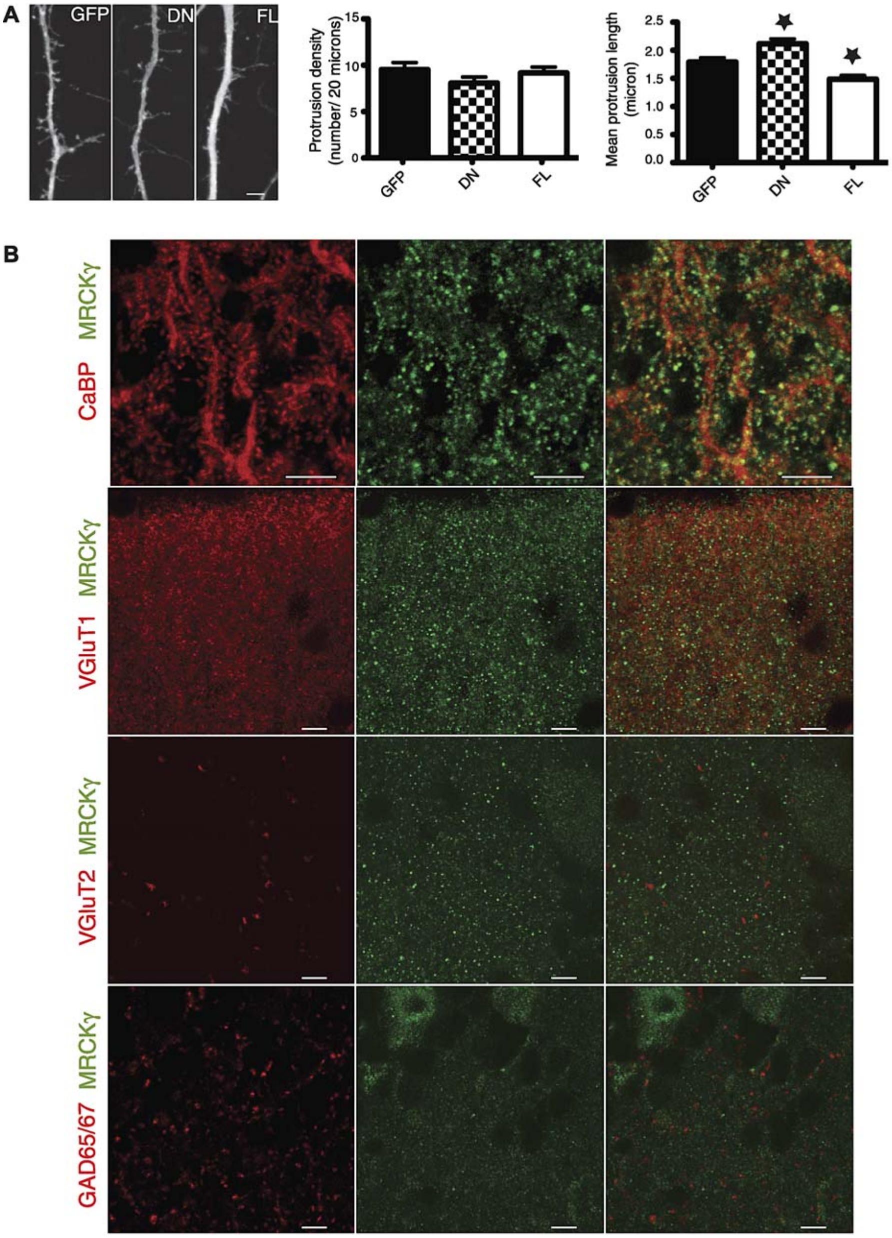

Figure 5. MRCKγ Modulates Dendritic Spine Morphogenesis and Is Localized to Parallel Fiber/Purkinje Cell Spines

(A) Primary cortical cultures were imaged at DIV14 after transfection with either GFP alone or in conjugation with MRCKγ lacking the kinase domain (DN) or the full-length MRCKγ kinase (FL) (left panel, scale bar indicates 10 μm). Mean protrusion density was not significantly different between the three conditions (middle), but significant changes in mean protrusion length were observed (right panel, asterisk [*] indicates $p < 0.05$ compared to GFP).

(B) Immunofluorescence labeling shows the localization of MRCKγ (green) in Purkinje cell spines (calbindin, red) and its colocalization with VgluT1, a marker of parallel fiber synapses, but not with VgluT2 or GAD65/67, markers of climbing fiber or of inhibitory synapses respectively. Scale bars indicate 5 μm.

doi:10.1371/journal.pbio.1000083.g005

BAI receptors or GABA-B receptors. In this regard, it is interesting to note that the GABA-B receptor 1 contains a CCP module in its extracellular domain. This module is also found in proteins of the complement cascade, which have recently been shown to be involved in synapse development [44]. These proteins, and the majority of the remaining proteins identified in this study, are specifically expressed in Purkinje cells within the cerebellum (see Results). Since cerebellar granule cells also receive excitatory inputs from mossy fibers, we can conclude that, even within the cerebellum, the synaptic codes for specific synapse types must be quite distinct. This supports the results of expression analysis of proteins identified in bulk synapse preparations showing that receptors and other upstream signaling molecules have a highly variable expression pattern in the vertebrate brain [17]. Taken together, these data indicate that very different sets of molecules must define different excitatory synapse types.

Although our approach employed the expression of a fusion of GluRδ2 with EGFP in a specific cell type, this basic approach can readily be adapted to characterize a wide variety of synapse types, given the wide range of affinity tags that are now available and the hundreds of BAC vectors that can be used to target expression to specific neurons (http://www.gensat.org). We anticipate that these additional studies of the biochemical diversity of synapses will be critical for understanding the development and function of specific CNS circuits and their dysfunction in disease [45,46].

Materials and Methods

Animals. All experiments using animals were performed according to protocols approved by the Institutional Animal Care and Use Committee at the Rockefeller University. Both the Pcp2/eGFP and the Pcp2/VGluRδ2 transgenics were bred on the FVB background, and littermates were used as wild-type controls.

Preparation of PSDs and affinity purification. Ten cerebella from adult mice were used for the preparation of a crude synaptosome fraction P2 as presented in Figure 2A (based on previously published protocols [47]). The solution used as a homogenization and resuspension buffer contained 0.32 M sucrose, 5 mM HEPES, 0.1 mM EDTA (pH 7.3), and a protease inhibitor cocktail (Sigma). P2 was then solubilized 30 min at 4 °C using a final concentration of 0.5% Triton X-100. The cleared solubilized fraction was separated by gravity flow on a gel-filtration column (Sephacryl S1000 Superfine; GE Healthcare) prepared using a solution containing 2 mM $CaCl_2$, 132 mM NaCl, 3 mM KCl, 2 mM $MgSO_4$, 1.2 mM NaH_2PO_4, 10 mM HEPES, and 0.5% Triton X-100 (pH 7.4). 2-ml fractions were collected, and aliquots were used for protein dosage using the BCA Protein assay kit (Pierce Biotechnology). Calibration of the gel-filtration column was performed using the gel-filtration HMW calibration kit (GE Healthcare).

Pooled fractions from the column were used for affinity purification of tagged PSDs. Dynabeads M-270 epoxy beads (Dynal) were conjugated using 15 μg of affinity-purified goat anti-GFP antibody per milligram of beads [22]; 6 mg of beads were used for affinity purification of pooled synaptic fractions from ten cerebella during 1 h at 4 °C. Beads were then washed in 2 mM $CaCl_2$, 300 mM NaCl, 3 mM KCl, 2 mM $MgSO_4$, 1.2 mM NaH_2PO_4, 10 mM HEPES, and 0.5% Triton X-100. Purified complexes were finally eluted in 0.5 N NH_4OH, 0.5 mM EDTA for 20 min, dried, and then resuspended in the desired volume of protein electrophoresis sample buffer. Biochemical preparations and affinity purifications were performed in parallel for each genotype, starting with ten cerebella each. For MS analysis, samples from several successive experiments were pooled.

Mass spectrometry analysis. Following immunopurification, the isolated proteins were resolved by 1-D SDS-PAGE and stained with Coomassie Blue (GelCode Blue; Pierce). As proteins stain with varied efficiency, for each sample (from the 30- and 50-mice preparations), the complete gel was subjected to mass spectrometric analysis. Each entire gel lane was cut into 66 × 1 mm sections. The 1-mm sections were combined in approximately 30 samples, and proteins were digested with 12.5 ng/μl sequencing-grade modified trypsin (Promega). The resulting peptides were extracted on reverse-phase resin (Poros 20 R2; PerSeptive Biosystems) and eluted with 50% (v/v) methanol, 20% (v/v) acetonitrile, and 0.1% (v/v) trifluoroacetic acid containing 2,5-dihydroxybenzoic acid (2,5-DHB; 1:3 v/v saturated matrix solution in elution solution). Samples were subjected to matrix-assisted laser desorption/ionization (MALDI) quadrupole/time-of-flight (QqTOF) MS and MALDI ion trap (MALDI-IT) tandem MS (MS/MS) analyses using an in-house–built MALDI interface coupled to a Qq-TOF instrument (QqTOF Centaur; Sciex) and an ion trap (LCQDECAXP^{PLUS}; Finnigan) as described [22,48,49]. XProteo computer algorithm (http://www.xproteo.com) was used to search the peptide fingerprint data and collision-induced dissociation (CID) MS/MS data in the NCBI database (see Text S1). Due to the limited amount of samples, all MALDI-IT CID MS/MS spectra were carefully acquired and interpreted manually. A MS/MS hypothesis-driven approach on isolates from control Pcp2/eGFP transgenic mice was used to probe for the specificity of the proteins copurified with VGluRδ2 (Text S1).

Dendritic spine morphometric analysis. The MRCKγ cDNA was amplified from cerebellar cDNA. The MRCKγDN construct was obtained by deleting the sequence encoding for amino acids 1–426, and by replacing it with ATG. MRCKγ and eGFP cDNAs were subcloned in the bidirectional Tet-responsive vector pBI (Clontech).

Primary neuronal cultures were prepared from E15 mouse embryos (Swiss strain). Cortices were dissected and triturated using a fire-polished Pasteur pipette and 0.05% trypsin. Neurons were plated on poly-D-lysine and laminin-coated coverslips at a density of 1.5×10^5 cells/cm^2 and cultured in neurobasal medium supplemented with 2% B27 supplement, 0.5 mM glutamine, and antibiotics. Transfections were performed at DIV7 with a 1:1 ratio of a tTA-expressing plasmid and the bidirectional vector containing GFP (with or without the kinases) using Lipofectamine 2000 according to the manufacturer's instructions (Invitrogen).

Dendrites of transfected neurons were imaged using a confocal microscope and a 63× objective with a 5× zoom. Quantifications of protrusion density and length were performed using the NeuronJ plugin and the ImageJ software on several dendrites per neuron (at least five different cells per transfection condition, four independent experiments). A total of 1,029, 861, and 950 protrusions were counted and measured for the GFP, DN, and FL transfections, respectively. Statistical analysis was performed using the GraphPad Prism software.

Supporting Information

Figure S1. Construction of a Fusion between Venus and GluRδ2 (VGluRδ2)

(A) Venus was fused on the N-terminal extracellular part of GluRδ2 (top left panel). A GluRδ2-positive band was detected in protein extracts from VGluRδ2-transfected HEK293 cells, but not in extracts from Venus-transfected cells (bottom left panel). The band was at the expected size (about 140 kDa), higher than the endogenous GluRδ2 detected in cerebellar extracts. Immunofluorescence using an anti-GFP antibody detected the extracellular Venus in VGluRδ2-transfected cells in nonpermeabilizing conditions (red, right panels), showing the proper topography of the tagged receptor.
(B) The correct modification of the Pcp2 BAC with the VGluRδ2 construct was checked by Southern blot (left panel, probe shown in [C], BAC DNA digested with EcoRI) and pulse-field gel electrophoresis (right panel, BAC DNA digested with SpeI), before injection in mouse oocytes.
(C) Schematic diagram of the BAC containing the Pcp2 gene, known to be expressed specifically in Purkinje cells. The VGluRδ2 cDNA was placed at the level of the Pcp2 ATG. The arrow indicates the promoter region.

Found at doi:10.1371/journal.pbio.1000083.sg001 (463 KB AI).

Figure S2. VGluRδ2 Is Fractionated Similarly to the Wild-Type GluRδ2 Receptor Using a Classical Synaptosome Preparation

Fractions obtained using the protocol of Dunkley et al. [47] for synaptosome preparation were probed for excitatory synapse markers (GluRδ2, PSD95), the inhibitory synapse marker GABA(A)Rα1, the endoplasmic reticulum marker BiP, and the mitochondrial marker COX. VGluRδ2 was detected using an anti-GFP antibody.

Found at doi:10.1371/journal.pbio.1000083.sg002 (498 KB AI).

Figure S3. Immunoelectron Micrograph of Affinity-Purified PSDs from VGluRδ2 Cerebella Labeled with an Anti-PSD95 Antibody

Found at doi:10.1371/journal.pbio.1000083.sg003 (9.05 MB AI).

Figure S4. Example of the Mass Spectrometric Strategy Utilized for Protein Identification and Confirmation, Illustrated for PSD93 and PSD95

(A) Following in-gel digestion with trypsin, the mixture of peptides was analyzed by MALDI QqToF MS. The m/z values of the [M+H]+ peptides were searched in the NCBI database using the XProteo software, and PSD93 and PSD95 were the first two hits with high scores. The lists of putative peptides generated by the XProteo software are shown, and their presence in the MALDI QqToF MS is indicated. T, trypsin peptides.
(B) The identity of the proteins was confirmed using MALDI-IT CID MS/MS analyses, and their specificity of isolation was investigated using a hypothesis-driven tandem MS approach on preparations from Pcp2/eGFP transgenic mice (GFP). Examples of results from MS/MS analyses on peptides of both high- and low-signal-to-noise ratios are shown.

Found at doi:10.1371/journal.pbio.1000083.sg004 (1.55 MB TIF).

Figure S5. The Analysis of Internexin and Camk2b in Immunoaffinity Purifications of VGluRδ2 Exemplifies the Identification and Confirmation of Proteins That Were Not Assigned a Score after the Database Search Using the XProteo Software

(A) Internexin and Camk2b peptides were both observed following MALDI QqToF MS analysis; however, only internexin received an XProteo database search score ($d' = 6$).
(B) The presence of both internexin and Camk2b was confirmed using MALDI-IT CID MS/MS analyses.

Found at doi:10.1371/journal.pbio.1000083.sg005 (868 KB TIF).

Figure S6. Examples of Spectra Obtained for Low-Confidence Candidates

Representative MALDI-IT CID MS/MS spectra are shown for Atp1a1 and Ncoa7. MALDI QqToF MS data and list of putative peptides are illustrated for Ptprm. The peaks attributed to Ptprm are shown with orange arrowheads. This portion of the gel contained multiple proteins. Light blue and dark blue dots indicate selected peaks attributed to Fodrin alpha chain and traces of GluRδ2, respectively. GluRδ2 was primarily identified in another gel band. Grey dot indicates a heavy labeled GluRδ2 peptide, spiked in all samples containing GluRδ2.

Found at doi:10.1371/journal.pbio.1000083.sg006 (823 KB TIF).

Table S1. List of Proteins Identified with Higher Confidence in the Immunoisolates of Venus-Tagged GluRδ2

Functional category, expression in Purkinje cells (PCs), and previous identification in PSD preparations (@PSD) are given.
(a) Reference numbers in this column refer to the list in Text S1.
(b) From reference [16]. Y indicates that the protein is detected; N, not detected; and I, the isoform is detected.

Found at doi:10.1371/journal.pbio.1000083.st001 (27 KB XLS).

Table S2. List of Proteins Identified in the Immunoisolates of Venus-Tagged GluRδ2 with Lower Levels of Confidence as Judged by Mass Spectrometry

Functional category, expression in Purkinje cells (PCs), and previous identification in PSD preparations (@PSD) are given.
(a) Reference numbers in this column refer to the list in Text S1.
(b) From reference [16].
Y indicates that the protein is detected; N, not detected; and I, the isoform is detected.

Found at doi:10.1371/journal.pbio.1000083.st002 (26 KB XLS).

Table S3. List of Proteins Identified in the Immunoisolates of Venus-Tagged GluRδ2

Results are shown of two replicate experiments from either 30 or 50 mice. The detection and confirmation of the proteins through MS and MS/MS analyses are indicated for both experiments. The sequence coverage, number of peptides, and scores obtained from the analysis of the MALDI QqToF MS spectra are given for the 50-mice experiment. The number and sequences of peptides confirmed by MALDI-IT CID MS/MS analyses are shown for each protein. The presence of these proteins in the control experiment, as judged by hypothesis-driven MS/MS analyses, is indicated. When the presence or absence of the protein could not be judged conclusively, due to either depletion of the sample or inconclusive fragmentation, the entry is marked as not available (n/a). n/o (not observed) in the score column refers to the proteins (MS) or peptides (MS/MS) that were not assigned a d′ value from the database search using the XProteo software.

Found at doi:10.1371/journal.pbio.1000083.st003 (57 KB XLS).

Table S4. List of Proteins Identified in the Immunoisolates of Venus-Tagged GluRδ2 with Lower Levels of Confidence as Judged by Mass Spectrometry

Results are shown from two replicate experiments from either 30 or 50 mice. The detection and confirmation of the proteins through MS and MS/MS analyses is indicated for both experiments. The sequence coverage, number of peptides, and scores obtained from the analysis of the MALDI QqToF MS spectra are given for the 50-mice experiment; a caret (∧) indicates a score obtained only after searching manually in the MS spectrum for peptides that could correspond to the protein of interest. The number and sequences of peptides confirmed by MALDI-IT CID MS/MS analyses are shown for each protein. Several proteins were not observed (n/o) at the MS analysis stage, but were identified from MS/MS analyses (not available [n/a]). The presence of these proteins in the control experiment, as judged by hypothesis-driven MS/MS analyses, is indicated. When the presence or absence of the protein could not be judged conclusively, due to either depletion of sample or inconclusive fragmentation, the entry is marked as not available (n/a). n/o (not observed) in the score column refers to the proteins (MS) or peptides (MS/MS) that were not assigned a d′ value from the database search using the XProteo software.

Found at doi:10.1371/journal.pbio.1000083.st004 (28 KB XLS).

Text S1. Supplementary Materials and Methods, and Supplementary References

Found at doi:10.1371/journal.pbio.1000083.sd001 (78 KB DOC).

Acknowledgments

We thank Pr. Cornelia Bargmann and Dr. Anne Schaefer for critical reading of the manuscript and helpful discussions. We also thank the Bioimaging facility at the Rockefeller University, in particular Helen Shio for electron microscopy analysis, and Alison North. We thank Kasia Losos for injection of transgenics, Jie Xing, and Wendy Lee for technical assistance. We thank Dr. Myriam Heiman for help with the goat anti-GFP serum affinity-purification and Pr. Chugh for the anti-Neph1 antibody.

Author contributions. FS generated the transgenic mice and performed immunofluorescence studies and functional analysis of MRCKγ. FS and EH performed the biochemical purifications of postsynaptic densities and their western blot analysis. IMC optimized the bead conjugation protocol and performed MS analysis. FS and NH prepared the manuscript. FS, IMC, EH, BTC, and NH discussed the experiments, the data, and the manuscript.

Funding. FS was supported by a fellowship from the Human Frontier Science Program Organization, and IMC by The Rockefeller University Women and Science Fellowship CEN5300379. This work was supported by grants from the Simons Foundation and National Institutes of Health grants RR00862 (BTC) and RR02220 (BTC). The funders had no role in study design, data collection and analysis, decision to publish, or preparation of the manuscript.

Competing interests. The authors have declared that no competing interests exist.

References

1. Sperry RW (1963) Chemoaffinity in the orderly growth of nerve fiber patterns and connections. Proc Natl Acad Sci U S A 50: 703–710.
2. Benson DL, Colman DR, Huntley GW (2001) Molecules, maps and synapse specificity. Nat Rev Neurosci 2: 899–909.
3. Craig AM, Boudin H (2001) Molecular heterogeneity of central synapses: afferent and target regulation. Nat Neurosci 4: 569–578.
4. Landsend AS, Amiry-Moghaddam M, Matsubara A, Bergersen L, Usami S, et al. (1997) Differential localization of delta glutamate receptors in the rat cerebellum: coexpression with AMPA receptors in parallel fiber-spine synapses and absence from climbing fiber-spine synapses. J Neurosci 17: 834–842.
5. Ango F, di Cristo G, Higashiyama H, Bennett V, Wu P, et al. (2004) Ankyrin-based subcellular gradient of neurofascin, an immunoglobulin family protein, directs GABAergic innervation at purkinje axon initial segment. Cell 119: 257–272.
6. Shen K, Fetter RD, Bargmann CI (2004) Synaptic specificity is generated by the synaptic guidepost protein SYG-2 and its receptor, SYG-1. Cell 116: 869–881.
7. Ango F, Wu C, Van der Want JJ, Wu P, Schachner M, et al. (2008) Bergmann glia and the recognition molecule CHL1 organize GABAergic axons and direct innervation of Purkinje cell dendrites. PLoS Biol 6: e103. doi:10.1371/journal.pbio.0060103
8. Jorntell H, Hansel C (2006) Synaptic memories upside down: bidirectional plasticity at cerebellar parallel fiber-Purkinje cell synapses. Neuron 52: 227–238.
9. Cotman CW, Banker G, Churchill L, Taylor D (1974) Isolation of postsynaptic densities from rat brain. J Cell Biol 63: 441–455.
10. Cohen RS, Blomberg F, Berzins K, Siekevitz P (1977) The structure of postsynaptic densities isolated from dog cerebral cortex. I. Overall morphology and protein composition. J Cell Biol 74: 181–203.
11. Walikonis RS, Jensen ON, Mann M, Provance DW Jr, Mercer JA, et al. (2000) Identification of proteins in the postsynaptic density fraction by mass spectrometry. J Neurosci 20: 4069–4080.
12. Cho KO, Hunt CA, Kennedy MB (1992) The rat brain postsynaptic density fraction contains a homolog of the Drosophila discs-large tumor suppressor protein. Neuron 9: 929–942.
13. Peng J, Kim MJ, Cheng D, Duong DM, Gygi SP, et al. (2004) Semi-

quantitative proteomic analysis of rat forebrain postsynaptic density fractions by mass spectrometry. J Biol Chem 279: 21003–21011.
14. Cheng D, Hoogenraad CC, Rush J, Ramm E, Schlager MA, et al. (2006) Relative and absolute quantification of postsynaptic density proteome isolated from rat forebrain and cerebellum. Mol Cell Proteomics 5: 1158–1170.
15. Husi H, Ward MA, Choudhary JS, Blackstock WP, Grant SG (2000) Proteomic analysis of NMDA receptor-adhesion protein signaling complexes. Nat Neurosci 3: 661–669.
16. Collins MO, Husi H, Yu L, Brandon JM, Anderson CN, et al. (2006) Molecular characterization and comparison of the components and multiprotein complexes in the postsynaptic proteome. J Neurochem 97 Suppl 1: 16–23.
17. Emes RD, Pocklington AJ, Anderson CN, Bayes A, Collins MO, et al. (2008) Evolutionary expansion and anatomical specialization of synapse proteome complexity. Nat Neurosci 11: 799–806.
18. Ito M (2001) Cerebellar long-term depression: characterization, signal transduction, and functional roles. Physiol Rev 81: 1143–1195.
19. Polleux F, Lauder JM (2004) Toward a developmental neurobiology of autism. Ment Retard Dev Disabil Res Rev 10: 303–317.
20. Takayama C, Nakagawa S, Watanabe M, Mishina M, Inoue Y (1996) Developmental changes in expression and distribution of the glutamate receptor channel delta 2 subunit according to the Purkinje cell maturation. Brain Res Dev Brain Res 92: 147–155.
21. Vinade L, Chang M, Schlief ML, Petersen JD, Reese TS, et al. (2003) Affinity purification of PSD-95-containing postsynaptic complexes. J Neurochem 87: 1255–1261.
22. Cristea IM, Williams R, Chait BT, Rout MP (2005) Fluorescent proteins as proteomic probes. Mol Cell Proteomics 4: 1933–1941.
23. Yuzaki M (2003) The delta2 glutamate receptor: 10 years later. Neurosci Res 46: 11–22.
24. Shiraishi Y, Mizutani A, Yuasa S, Mikoshiba K, Furuichi T (2004) Differential expression of Homer family proteins in the developing mouse brain. J Comp Neurol 473: 582–599.
25. Uemura T, Mori H, Mishina M (2004) Direct interaction of GluRdelta2 with Shank scaffold proteins in cerebellar Purkinje cells. Mol Cell Neurosci 26: 330–341.
26. Adams JC, Tucker RP (2000) The thrombospondin type 1 repeat (TSR) superfamily: diverse proteins with related roles in neuronal development. Dev Dyn 218: 280–299.
27. Sallee JL, Wittchen ES, Burridge K (2006) Regulation of cell adhesion by protein-tyrosine phosphatases: II. Cell-cell adhesion. J Biol Chem 281: 16189–16192.
28. Kosik KS, Donahue CP, Israely I, Liu X, Ochiishi T (2005) Delta-catenin at the synaptic-adherens junction. Trends Cell Biol 15: 172–178.
29. Shen K, Bargmann CI (2003) The immunoglobulin superfamily protein SYG-1 determines the location of specific synapses in C. elegans. Cell 112: 619–630.
30. Dityatev A, Schachner M (2006) The extracellular matrix and synapses. Cell Tissue Res 326: 647–654.
31. Leung T, Chen XQ, Tan I, Manser E, Lim L (1998) Myotonic dystrophy kinase-related Cdc42-binding kinase acts as a Cdc42 effector in promoting cytoskeletal reorganization. Mol Cell Biol 18: 130–140.
32. Dong JM, Leung T, Manser E, Lim L (2002) Cdc42 antagonizes inductive action of cAMP on cell shape, via effects of the myotonic dystrophy kinase-related Cdc42-binding kinase (MRCK) on myosin light chain phosphorylation. Eur J Cell Biol 81: 231–242.
33. Nimchinsky EA, Sabatini BL, Svoboda K (2002) Structure and function of dendritic spines. Annu Rev Physiol 64: 313–353.
34. Sheng M, Hoogenraad CC (2007) The postsynaptic architecture of excitatory synapses: a more quantitative view. Annu Rev Biochem 76: 823–847.
35. Koekkoek SK, Yamaguchi K, Milojkovic BA, Dortland BR, Ruigrok TJ, et al. (2005) Deletion of FMR1 in Purkinje cells enhances parallel fiber LTD, enlarges spines, and attenuates cerebellar eyelid conditioning in Fragile X syndrome. Neuron 47: 339–352.
36. Dindot SV, Antalffy BA, Bhattacharjee MB, Beaudet AL (2008) The Angelman syndrome ubiquitin ligase localizes to the synapse and nucleus, and maternal deficiency results in abnormal dendritic spine morphology. Hum Mol Genet 17: 111–118.
37. Allen KM, Gleeson JG, Bagrodia S, Partington MW, MacMillan JC, et al. (1998) PAK3 mutation in nonsyndromic X-linked mental retardation. Nat Genet 20: 25–30.
38. Di Paolo G, De Camilli P (2006) Phosphoinositides in cell regulation and membrane dynamics. Nature 443: 651–657.
39. Martin-Belmonte F, Gassama A, Datta A, Yu W, Rescher U, et al. (2007) PTEN-mediated apical segregation of phosphoinositides controls epithelial morphogenesis through Cdc42. Cell 128: 383–397.
40. Halstead JR, Jalink K, Divecha N (2005) An emerging role for PtdIns(4,5)P2-mediated signalling in human disease. Trends Pharmacol Sci 26: 654–660.
41. Voronov SV, Frere SG, Giovedi S, Pollina EA, Borel C, et al. (2008) Synaptojanin 1-linked phosphoinositide dyshomeostasis and cognitive deficits in mouse models of Down's syndrome. Proc Natl Acad Sci U S A 105: 9415–9420.
42. Berman DE, Dall'Armi C, Voronov SV, McIntire LB, Zhang H, et al. (2008) Oligomeric amyloid-beta peptide disrupts phosphatidylinositol-4,5-bisphosphate metabolism. Nat Neurosci 11: 547–554.
43. Dunah AW, Hueske E, Wyszynski M, Hoogenraad CC, Jaworski J, et al. (2005) LAR receptor protein tyrosine phosphatases in the development and maintenance of excitatory synapses. Nat Neurosci 8: 458–467.
44. Stevens B, Allen NJ, Vazquez LE, Howell GR, Christopherson KS, et al. (2007) The classical complement cascade mediates CNS synapse elimination. Cell 131: 1164–1178.
45. Serajee FJ, Nabi R, Zhong H, Mahbubul Huq AH (2003) Association of INPP1, PIK3CG, and TSC2 gene variants with autistic disorder: implications for phosphatidylinositol signalling in autism. J Med Genet 40: e119.
46. Kennedy MB (2000) Signal-processing machines at the postsynaptic density. Science 290: 750–754.
47. Dunkley PR, Heath JW, Harrison SM, Jarvie PE, Glenfield PJ, et al. (1988) A rapid Percoll gradient procedure for isolation of synaptosomes directly from an S1 fraction: homogeneity and morphology of subcellular fractions. Brain Res 441: 59–71.
48. Krutchinsky AN, Kalkum M, Chait BT (2001) Automatic identification of proteins with a MALDI-quadrupole ion trap mass spectrometer. Anal Chem 73: 5066–5077.
49. Krutchinsky AN, Zhang W, Chait BT (2000) Rapidly switchable matrix-assisted laser desorption/ionization and electrospray quadrupole-time-of-flight mass spectrometry for protein identification. J Am Soc Mass Spectrom 11: 493–504.

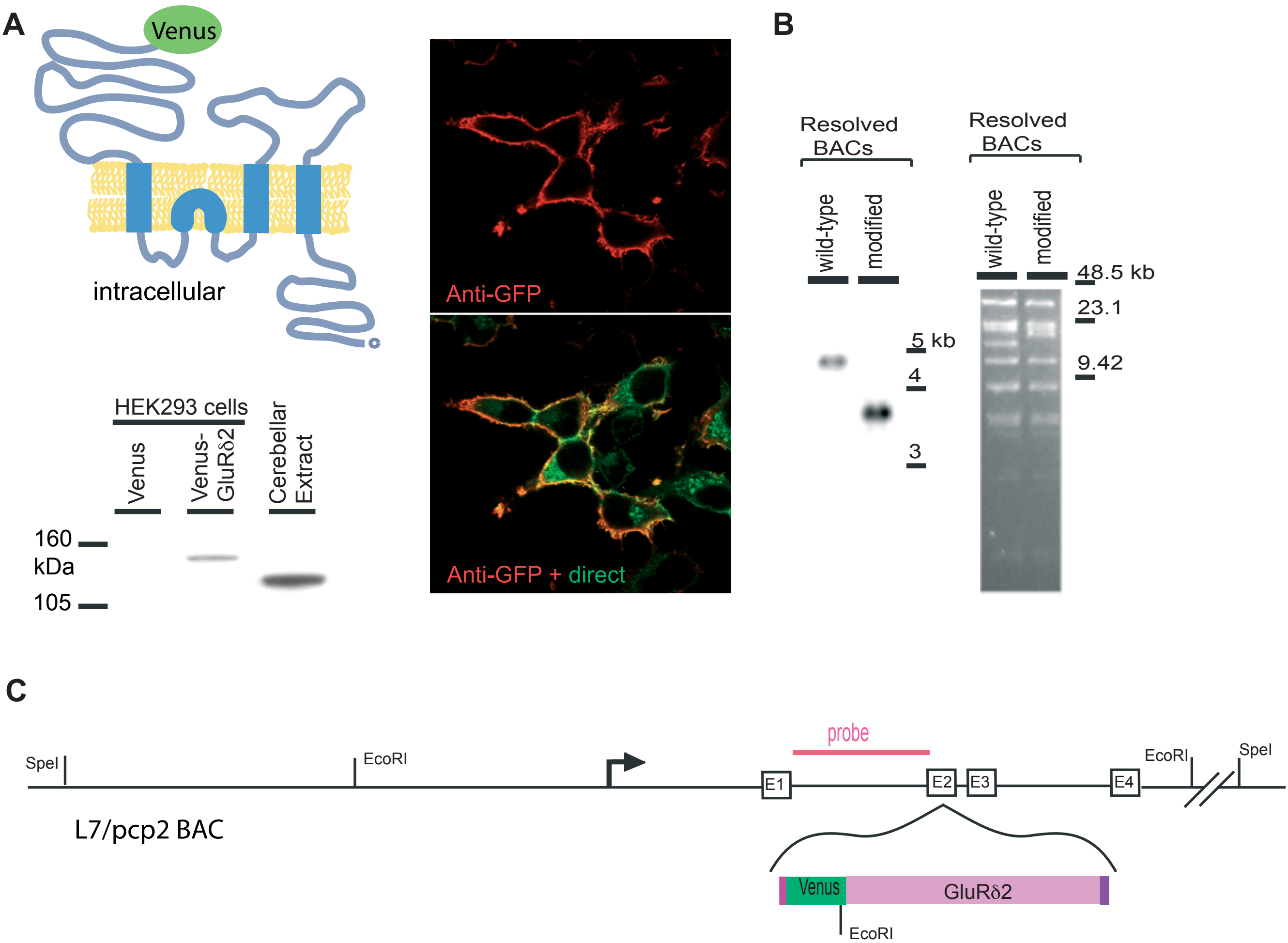

A
Venus
intracellular
HEK293 cells
Venus
Venus-GluRδ2
Cerebellar Extract
160
kDa
105
Anti-GFP
Anti-GFP + direct
B
Resolved BACs
wild-type
modified
5 kb
4
3
Resolved BACs
wild-type
modified
48.5 kb
23.1
9.42
C
probe
SpeI
EcoRI
E1
E2
E3
E4
EcoRI
SpeI
L7/pcp2 BAC
Venus
GluRδ2
EcoRI

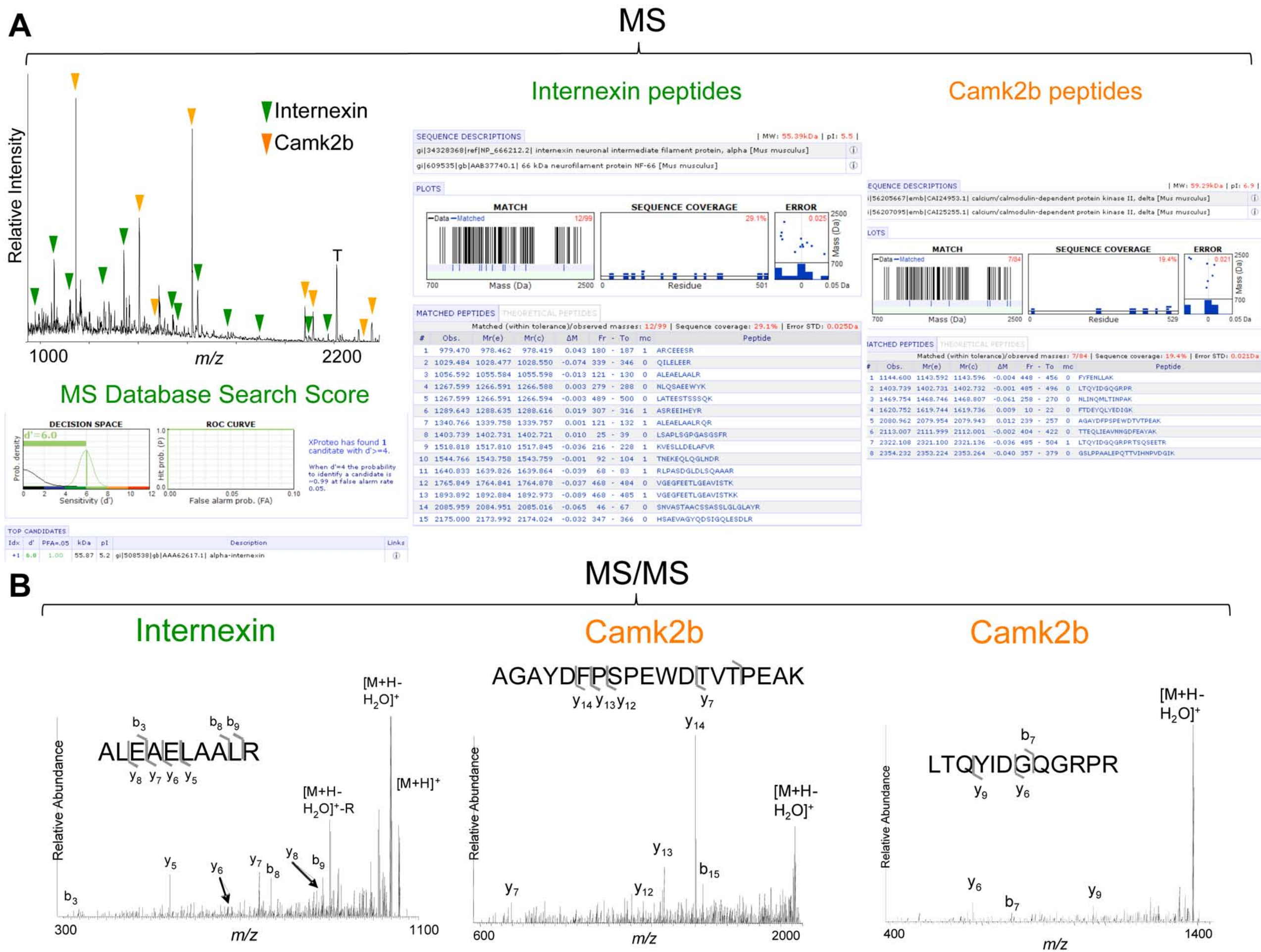

A
MS
Relative Intensity
Internexin
Camk2b
T
1000
m/z
2200
Internexin peptides
SEQUENCE DESCRIPTIONS
| MW: 55.39kDa | pI: 5.5 |
gi|34328368|ref|NP_666212.2| internexin neuronal intermediate filament protein, alpha [Mus musculus]
gi|609535|gb|AAB37740.1| 66 kDa neurofilament protein NF-66 [Mus musculus]
PLOTS
MATCH
SEQUENCE COVERAGE
ERROR
Mass (Da)
Residue
MATCHED PEPTIDES
THEORETICAL PEPTIDES
Matched (within tolerance)/observed masses: 12/99 | Sequence coverage: 29.1% | Error STD: 0.025Da
1 979.470 978.462 978.419 0.043 180 - 187 1 ARCEEESR
2 1029.484 1028.477 1028.550 -0.074 339 - 346 0 QILELEER
3 1056.592 1055.584 1055.598 -0.013 121 - 130 0 ALEAELAALR
4 1267.599 1266.591 1266.588 0.003 279 - 288 0 NLQSAEEWYK
5 1267.599 1266.591 1266.594 -0.003 489 - 500 0 LATEESTSSSQK
6 1289.643 1288.635 1288.616 0.019 307 - 316 1 ASREEIHEYR
7 1340.766 1339.758 1339.757 0.001 121 - 132 1 ALEAELAALRQR
8 1403.739 1402.731 1402.721 0.010 25 - 39 0 LSAPLSGPGASGSFR
9 1518.818 1517.810 1517.845 -0.036 216 - 228 1 KVESLLDELAFVR
10 1544.766 1543.758 1543.759 -0.001 92 - 104 1 TNEKEQLQGLNDR
11 1640.833 1639.826 1639.864 -0.039 68 - 83 1 RLPASDGLDLSQAAAR
12 1765.849 1764.841 1764.878 -0.037 468 - 484 0 VGEGFEETLGEAVISTK
13 1893.892 1892.884 1892.973 -0.089 468 - 485 1 VGEGFEETLGEAVISTKK
14 2085.959 2084.951 2085.016 -0.065 46 - 67 0 SNVASTAACSSASSLGLGLAYR
15 2175.000 2173.992 2174.024 -0.032 347 - 366 0 HSAEVAGYQDSIGQLESDLR
Camk2b peptides
SEQUENCE DESCRIPTIONS
| MW: 59.29kDa | pI: 6.9 |
gi|56205667|emb|CAI24953.1| calcium/calmodulin-dependent protein kinase II, delta [Mus musculus]
gi|56207095|emb|CAI25255.1| calcium/calmodulin-dependent protein kinase II, delta [Mus musculus]
Matched (within tolerance)/observed masses: 7/84 | Sequence coverage: 19.4% | Error STD: 0.021Da
1 1144.600 1143.592 1143.596 -0.004 448 - 456 0 FYFENLLAK
2 1403.739 1402.731 1402.732 -0.001 485 - 496 0 LTQYIDGQGRPR
3 1469.754 1468.746 1468.807 -0.061 258 - 270 0 NLINQMLTINPAK
4 1620.752 1619.744 1619.736 0.009 10 - 22 0 FTDEYQLYEDIGK
5 2080.962 2079.954 2079.943 0.012 239 - 257 0 AGAYDFPSPEWDTVTPEAK
6 2113.007 2111.999 2112.001 -0.002 404 - 422 0 TTEQLIEAVNNGDFEAYAK
7 2322.108 2321.100 2321.136 -0.036 485 - 504 1 LTQYIDGQGRPRTSQSEETR
8 2354.232 2353.224 2353.264 -0.040 357 - 379 0 GSLPPAALEPQTTVIHNPVDGIK
MS Database Search Score
DECISION SPACE
ROC CURVE
Sensitivity (d')
False alarm prob. (FA)
XProteo has found 1 canditate with d'>=4.
When d'=4 the probability to identify a candidate is ~0.99 at false alarm rate 0.05.
TOP CANDIDATES
+1 6.0 1.00 55.87 5.2 gi|508538|gb|AAA62617.1| alpha-internexin
B
MS/MS
Internexin
ALEAELAALR
Relative Abundance
300
m/z
1100
[M+H-H2O]+
[M+H]+
[M+H-H2O]+-R
Camk2b
AGAYDFPSPEWDTVTPEAK
600
m/z
2000
Camk2b
LTQYIDGQGRPR
400
m/z
1400

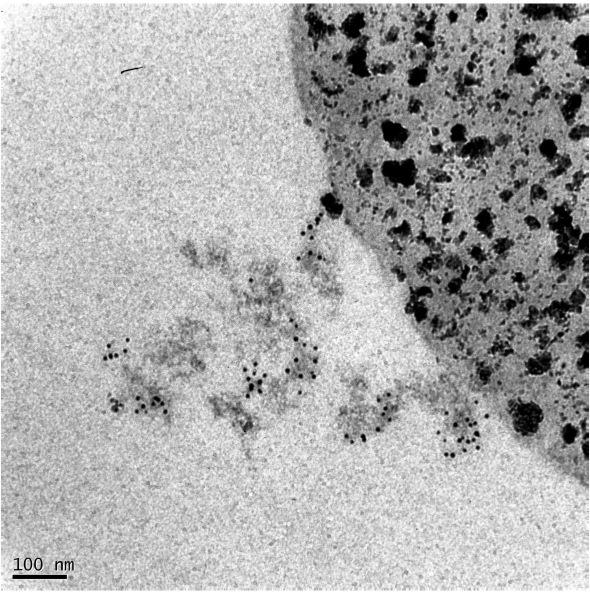
100 nm

Examples of MS/MS of low confidence candidates

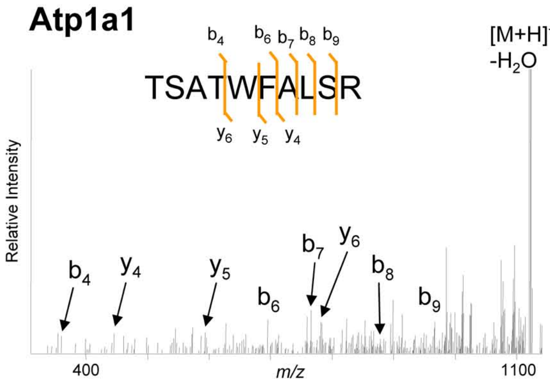

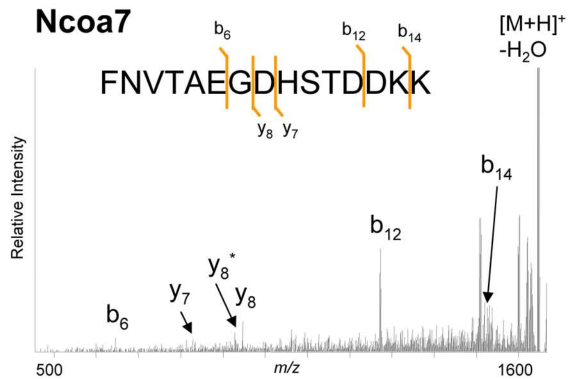

Examples of MS of low confidence candidates

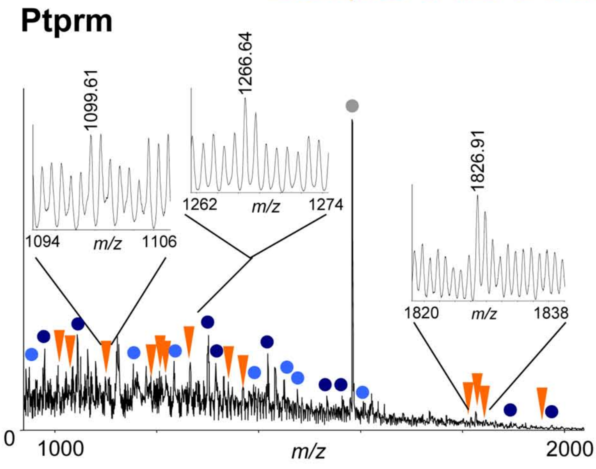

Putative Ptprm peptides

MATCHED PEPTIDES | THEORETICAL PEPTIDES

Matched (within tolerance)/observed masses: 15/22 | Sequence coverage

#	Obs.	Mr(e)	Mr(c)	ΔM	Fr - To	mc	P
1	1015.517	1014.509	1014.550	-0.041	1414 - 1422	0	TVDVFHAVK
2	1033.463	1032.455	1032.459	-0.003	1169 - 1176	0	SLYYDMNK
3	1042.572	1041.565	1041.564	0.000	459 - 467	0	LILMNPEGR
4	1099.615	1098.608	1098.619	-0.011	218 - 226	0	LWLQGIDVR
5	1157.575	1156.567	1156.543	0.024	818 - 828	0	SVSSPSSFTMK
6	1266.640	1265.633	1265.607	0.025	1118 - 1128	0	EGVVDIYNCVR
7	1329.600	1328.592	1328.593	-0.000	1011 - 1020	0	YWPDDTEIYK
8	1329.600	1328.592	1328.633	-0.041	1217 - 1227	1	NRCMDILPPDR
9	1340.709	1339.701	1339.714	-0.013	241 - 252	0	FIASFNVVNTTK
10	1345.696	1344.688	1344.740	-0.052	107 - 119	0	SNAAPGLLNVYVK
11	1365.670	1364.662	1364.673	-0.010	570 - 582	0	GFGPPATNQFTTK
12	1821.837	1820.829	1820.854	-0.025	522 - 538	0	AVSSFDPEIDLSNQSGR
13	1826.910	1825.902	1825.878	0.024	1102 - 1117	0	TGCFIVIDIMLDMAER
14	1830.833	1829.825	1829.875	-0.049	1342 - 1355	0	MVQQFQFLGWPMYR
15	1941.852	1940.844	1940.836	0.008	91 - 106	0	ENDTHCIDFHYFVSSK

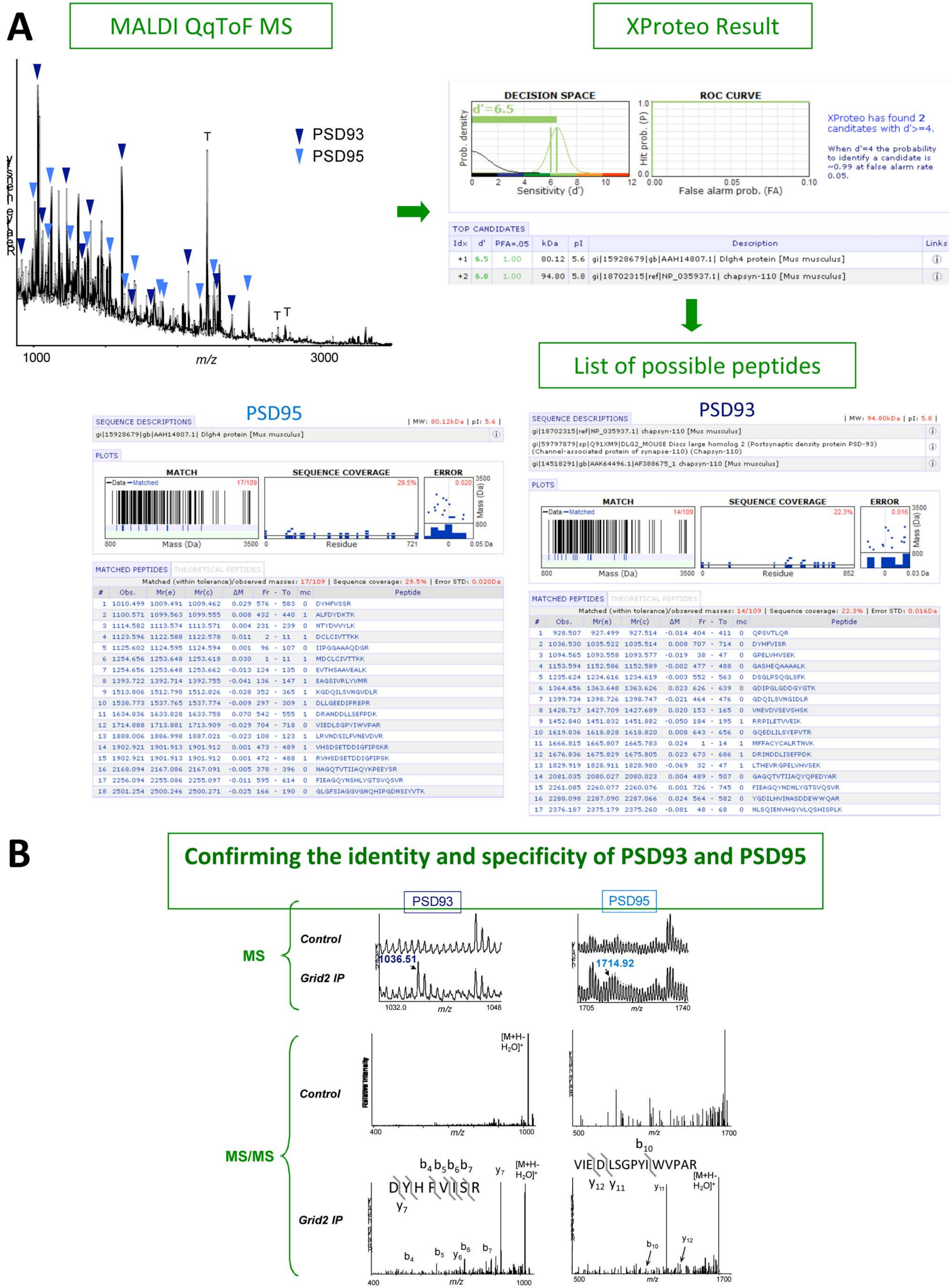
A
MALDI QqToF MS
XProteo Result
PSD93
PSD95
m/z
1000
3000
DECISION SPACE
ROC CURVE
d'=6.5
Prob. density
Sensitivity (d')
Hit prob. (P)
False alarm prob. (FA)
XProteo has found 2 canditates with d'>=4.
When d'=4 the probability to identify a candidate is ~0.99 at false alarm rate 0.05.
TOP CANDIDATES
Idx d' PFA=.05 kDa pI Description Links
+1 6.5 1.00 80.12 5.6 gi|15928679|gb|AAH14807.1| Dlgh4 protein [Mus musculus]
+2 6.0 1.00 94.80 5.8 gi|18702315|ref|NP_035937.1| chapsyn-110 [Mus musculus]
List of possible peptides
PSD95
PSD93
SEQUENCE DESCRIPTIONS
PLOTS
MATCH
SEQUENCE COVERAGE
ERROR
MATCHED PEPTIDES
B
Confirming the identity and specificity of PSD93 and PSD95
MS
MS/MS
Control
Grid2 IP
1036.51
1714.92
m/z
DYHFVISR
VIEDLSGPYIWVPAR
[M+H-H2O]+
Relative intensity

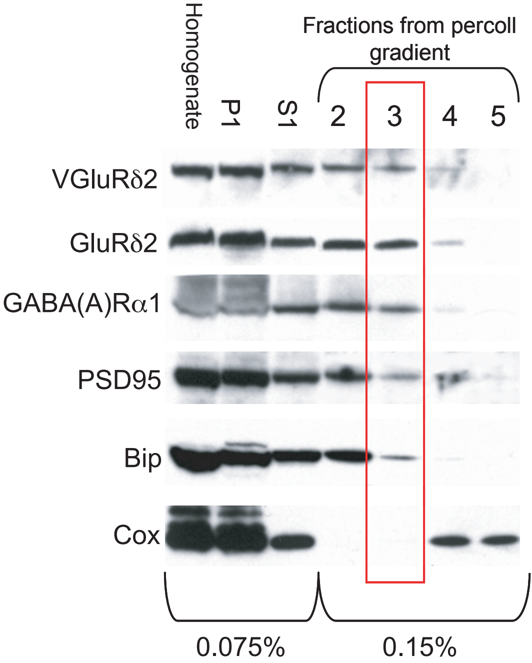
Homogenate
P1
S1
Fractions from percoll gradient
2
3
4
5
VGluRδ2
GluRδ2
GABA(A)Rα1
PSD95
Bip
Cox
0.075%
0.15%

Table 1: Proteins isolated via VGluRδ2

Category	Protein	Description	gi #	Function	Expression in PCs (a)	@ PSD (b)
TAG	YFP	Venus				
Tagged protein	GluRδ2	glutamate receptor, ionotropic, delta 2	6680091	Receptors, channels and ion transport	Y (1,3)	Y
Isolated proteins (Mus Musculus)	Shank2	SH3/ankyrin domain gene 2	28804747	Scaffolds and adaptors	Y (1,4)	Y
	Shank1	PREDICTED: SH3 and multiple ankyrin repeat domains 1 isoform 3	82905881	Scaffolds and adaptors	Y (4)	Y
	Homer3	homer-3	3834613	Scaffolds and adaptors	Y (1,2,5)	Y
	PSD95	Dlgh4 protein	15928679	Scaffolds and adaptors	Y (1,6)	Y
	PSD93	chapsyn-110	14518291	Scaffolds and adaptors	Y (1,7)	Y
	Jakmip1	gamma-aminobutyric acid (GABA-B) receptor binding protein	30409980	Scaffolds and adaptors	Y (1)	
	Grid2ip	glutamate receptor, ionotropic delta 2 (Grid2) interacting protein 1	19111166	Scaffolds and adaptors	Y (1,8)	
	AMPA2	glutamate receptor, ionotropic, AMPA2 (alpha 2)	85861224	Receptors, channels and ion transport	Y (1,2,9)	Y
	Gabbr1	GABA B receptor 1	131888529	Receptors, channels and ion transport	Y (1,2,10)	Y
	Plekha7	Plekha7 protein [Mus musculus]	54038521	Phospholipid metabolism and signaling	Y (1)	I
	MRCK gamma	CDC42-binding protein kinase gamma (MRCK gamma) (DMPK-like gamma)	81174937	Phospholipid metabolism and signaling	Y (our data)	Y
	Itpr1	inositol 1,4,5-triphosphate receptor 1	146198792	Phospholipid metabolism and signaling	Y (1,2,5)	Y
	Anxa6	Annexin A6 protein	13542782	Phospholipid metabolism and signaling	Y (1, 11)	I
	4930407I10Rik	PREDICTED: hypothetical protein	94399886	Others	no data	
	Dnahc8	axonemal dynein heavy chain 8	13310482	Motor proteins	Y (1)	
	Dnahc12	PREDICTED: dynein, axonemal, heavy chain 12	149265372	Motor proteins	no data	
	Cep152	centrosomal protein 152	82885523	Motor proteins	no data	
	Zwint	SNAP25 interacting protein 30	22028168	Membrane trafficking	Y (1)	Y
	P140	PREDICTED: similar to p130Cas-associated protein (p140) (SNAP-25-interacting protein) (SNIP)	94390735	Membrane trafficking	no data	Y
	RPTPmam4	brain RPTPmam4 isoform 1	13378306	Kinases and phosphatases	no data	I
	Camk2b	Camk2b protein	51480474|	Kinases and phosphatases	Y (1, 12)	Y
	Camk2a	calcium/calmodulin-dependent protein kinase II alpha isoform 2	28916677	Kinases and phosphatases	Y (1,2,12)	Y

Table 1: Proteins isolated via VGluRδ2

Category	Protein	Description	gi #	Function	Expression in PCs (a)	@ PSD (b)
	Synaptopodin isoform 2	PREDICTED: synaptopodin isoform 2	94404501	GTPases and regulators	no data	
	Gm941	PREDICTED: hypothetical protein	82995169	GTPases and regulators	Y (our data)	
	CAST2 beta	Rab6ip2/CAST2 beta	32478657	GTPases and regulators	no data	I
	Mtap6	neuronal-STOP protein	3171934	Cytoskeleton	Y (1)	Y
	Ina	internexin neuronal intermediate filament protein, alpha	17390900	Cytoskeleton	Y (1, 13)	Y
	HSP 84	Heat shock protein HSP 90-beta (HSP 84) (Tumor-specific transplantation 84 kDa antigen) (TSTA)	123681	Chaperonne	Y (1)	Y
	Lama1	laminin, alpha 1	117168301	Cell adhesion and matrix	no data	
	BC022960	PREDICTED: similar to periphilin 1 isoform 1	94408554	Cell adhesion and matrix	no data	
	Catenin delta-2	PREDICTED: similar to Catenin delta-2 (Neural plakophilin-related ARM-repeat protein) (NPRAP) (Neurojungin)	94398572	Cell adhesion and matrix	Y (1)	Y
Likely Contami- - nants	Myo18a	Myo18a protein	28436851	Motor proteins	Y (1)	Y
	Myo7b	myosin VIIb	14161694	Motor proteins	no data	Y
	Cingulin	PREDICTED: similar to Cingulin	94371022	Motor proteins	no data	
	Spnb2	spectrin beta 2	56206997	Cytoskeleton	no data	I
	Actb	actin, beta, cytoplasmic	74213524	Cytoskeleton	Y (1,2)	Y

Table 2: Proteins isolated via VGluRδ2

Category	Protein	Description	gi #	Function	Expression in PCs (a)	@ PSD (b)
Isolated proteins	Grik4	Glutamate receptor, ionotropic, kainate 4	109730793	Receptors, channels and ion transport	Y (2)	I
Mus	GluR3	GluR3	84781717	Receptors, channels and ion transport	Y (1,9)	Y
Musculus	GluR1	Glu receptor 1	227246	Receptors, channels and ion transport	Y (1,9)	Y
	Gabbr2	PREDICTED: similar to Gamma-aminobutyric acid type B receptor, subunit 2 precursor (GABA-B receptor 2)	94373276	Receptors, channels and ion transport	Y (1, 2, 10)	Y
	Bai3	brain-specific angiogenesis inhibitor 3	28628123	Receptors, channels and ion transport	Y (1)	Y
	Bai2	Brain-specific angiogenesis inhibitor 2 precursor	110278892	Receptors, channels and ion transport	Y (1)	I
	Atp6v1a	ATPase, H+ transporting, V1 subunit A	31560731	Receptors, channels and ion transport	Y (1)	Y
	Atp2a3	ATPase, Ca++ transporting, ubiquitous	31542159	Receptors, channels and ion transport	Y (1,14)	I
	Atp1a1	Atp1a1 protein	16307541	Receptors, channels and ion transport	Y (1)	Y
	Synj2	Synaptojanin-2 (Synaptic inositol-1,4,5-triphosphate 5-phosphatase 2)	37590481	Phospholipid metabolism and signalling	Y (1,15)	Y
	Synj1	Synaptojanin-1 (Synaptic inositol-1,4,5-triphosphate 5-phosphatase 1)	149268231	Phospholipid metabolism and signalling	Y (1)	Y
	Plb1	PREDICTED: similar to phospholipase B [Mus musculus]	94376138	Phospholipid metabolism and signalling	no data	
	4833417A11Rik	PREDICTED: similar to ATP-binding cassette, sub-family A, member 12 isoform a isoform 2	94363638	Phospholipid metabolism and signalling	no data	
	Setbp1	SETbinding protein	51890215	others	Y (1)	
	Ncoa7	Ncoa7 protein	50369666	others	Y (1)	
	Ant1	adenine nucleotide translocase-1	902008	others	Y (1)	
	Ranbp2	Ran-binding protein 2	10442646	Others	Y (1)	I
	LOC70950	hypothetical protein LOC70950	30794402	Motor proteins	no data	
	R-PTP-mu	Receptor-type tyrosine-protein phosphatase mu precursor (R-PTP-mu)	131570	Kinases and phosphatases	(1,our data)	I
	Mekk3	PREDICTED: similar to Mitogen-activated protein kinase kinase kinase 3 (MEKK 3)	33468949	Kinases and phosphatases	no data	
	Synaptopodin	synaptopodin	48428644	GTPases and regulators	no	
	Baiap2	Baiap2 protein	13879292	GTPases and regulators	(1, 20, our data)	
	Nesprin 2	similar to nesprin2	145699091	cytoskeleton	no data	

Table 2: Proteins isolated via VGluRδ2

Category	Protein	Description	gi #	Function	Expression in PCs (a)	@ PSD (b)
	LAMA2	laminin alpha 2 subunit precursor variant	62087424	Cell adhesion and matrix	no data	
	NEPH1	NEPH1	14572519	Cell adhesion and matrix	our data	
Likely contami -nants	spectrin alpha 2	PREDICTED: similar to Spectrin alpha chain, brain; (Alpha-II spectrin) (Fodrin alpha chain)	115496850	cytoskeleton	Y(1,2)	I
	mKIAA4061	mKIAA4061 protein = from Blast seacrh, homologue to spectrin domain with coiled-coils 1	60360496	cytoskeleton	no	
	LOC672116	PREDICTED: similar to zinc finger protein 616	94369146	others	no data	

Table 3: Proteins isolated viaVGluRδ2

Category	Protein	gi #	NCBI#	MS 30 mice	MS 50 mice	Sequence coverage (%)	Number of peptides	Score MS (d')	MS/MS 30 mice	MS/MS 50 mice	# peptides	Score MS/MS (d')	Peptide sequences	In control
TAG	YFP	6453571	CAB61435.1	Y	Y	46.2	13	6.5	Y	Y	2	n/o	GIDFKEDGNILGHK TIFFKDDGNYK LEYNYNSHNVYITADK FSVSGEGEGDATYGK	Y
Tagged protein	Grid2	6680091	NP_032193.1	Y	Y	28.8	29	16.2	Y	Y	9	22.9	RHPPTPPDPSGGLPR FIIFYDSEYDIR AASGFAFGSVPEHR GYGIALQHGSPYR YMDYSVGVLLR TAVGDLNQNEEILQTEK NSKPWQGGR TMSSIPYQPTPTLGLNLGNDPDR VVTEYAWQK	N
Isolated proteins (Mus Musculus)	Grid2ip	19111166	NP_579933	N	Y	14.3	16	5.1	N	Y	7	n/o	RPDEPPPR STFLHILAK LNSSFKGK FLDALSEQLGPR YQAFREAPGR ALDGLQREAMEELGK SCLGIFIPKK	N
	Homer3	3834613	AAC71025.1	Y	Y	39.8	13	15.3	Y	Y	3	9.8	VAELEAQVAVEPVR HALTVSYFYDATR EAPDTAER	N
	Shank1	82905881	XP_899334.1	N	Y	14.1	28	2.3	N	Y	7	1.3	FNPDATIWTAK FLEYVQLGTSDK TAAPEEPERLPLHVR SIGAAEDDRPYLAPPAMK GFFATESSFDPHHR SIDEGMFSAEPYLR HSKSIDEGMFSAEPYLR	N
	Shank2	28804747	BAC58120.1	Y	Y	21.5	25	10.7	Y	Y	2	n/o	LLDPSSPLALALSAR NSPAFLSTDLGDEDVGLGPPAPR	N
	PSD93	14518291	AAK64496.1	Y	Y	28.1	22	9.5	Y	Y	3	1.4	DYHFVISR GDQILSVNGIDLR INDDLISEFPDK	N
	PSD95	15928679	AAH14807.1	Y	Y	29.5	18	6.5	Y	Y	4	n/o	VIEDLSGPYIWVPAR DYHFVSSR DLLGEEDIPREPR ANDDLLSEFPDK	N
	Ina	17390900	AAH18383.1	Y	Y	29.1	15	6	Y	Y	8	n/o	ALEAELAALR VGEGFEETLGEAVISTK LPASDGLDLSQAAAR LSAPLSGPGASGSFR QILELEER TNEYKIIR EQLQGLNDR EYQDLLNVK	N
	Jakmip1	30409980	NP_848481.1	N	Y	9.4	9	n/o	N	Y	2	n/o	MQQEISELK	N

Table 3: Proteins isolated viaVGluRδ2													
Category	Protein	gi #	NCBI#	MS 30 mice	MS 50 mice	Sequence coverage (%)	Number of peptides	Score MS (d')	MS/MS 30 mice	MS/MS 50 mice	# peptides	Score MS/MS (d')	Peptide sequences	In control
													LQLQKEALDEQLSQAK	
	Gabbr1	131888529	NP_062312	Y	Y	8.6	7	n/o	Y	Y	7	n/o	DILPDYELK THPSATLHNPTR RDILPDYELK DDLSWSKTDK ELEKIIAEK EDIDVSILPQLEHCSSK RHPPTPPDPSGGLPR	n/a
	Mtap6	3171934	CAA75930.1	N	Y	10.1	12	n/o	N	Y	4	n/o	NKDSVPLAPAK AGPAWMVRR GPVTKEPHK TTEGPSATKPDDK	N
	CAST2 beta	32478657	AAP83581.1	N	Y	18.5	24	5.4	N	Y	1	n/o	EVLRENDLLR	N
	Cep152	82885523	XP_923083	N	Y				N	Y	7	n/o	TEFINR QQELAVAHR GPSCGALEPYK DMLRYIQESK CGDASCRHSGVLAK ETEFQACLDQSRK TPPRSLSAGAAESAGPSCSR	N
	Camk2a	28916677	NP_803126.1	Y	Y	24.8	11	6.8	Y	Y	3	n/o	AGAYDFPSPEWDTVTPEAK* FYFENLWSR ITQYLDAGGIPR	N
	Camk2b	51480474|	AAH80273.1	Y	Y	19.4	8	n/o	Y	Y	2	n/o	LTQYIDGQGRPR AGAYDFPSPEWDTVTPEAK*	N
	Catenin delta-2	94398572	XP_986270	N	N	n/a	n/a	n/a	N	Y	5	n/o	SGPALPPEGTLAR SYWSHK AAGQSFSQGTTGR SSHGKSYWSHK GWAEDVAGMAYALR	N
	Gm941	82995169	XP_894872	Y	Y	20.4	27	9	Y	Y	5	2.7	GPPELLPDAR DLPECISLVHVVVLK TFFPQQR APAPHGPAAAAAASR TPPAEGVAPRLYSTR	N
	MRCK gamma	81174937	Q80UW5	Y	Y	10.4	18	n/o	Y	Y	8	n/o	LELQSALEAEIR LQKMEASAR LGRGGLDDFR SLRMGSVFPR QSQALQQEVAELR EEVLCRLQEENQR NVGTQTLPTRPLDHQWK RPVSTGSDGLPGETDPLVK	N
	AMPA2	85861224	NP_038568	N	Y	5.9	8	n/o	N	Y	1	n/o	SAEPSVFVR	N
	Cingulin	94371022	XP_980833	N	Y	15.1	7	3.4	Y	Y	7	n/o	TLPHEQR KEHCGTVNR EEEGNLAAAKR ATKQELLQLR DWASEAEKNSGGLSR VASETEAMVLGQR	Y

Table 3: Proteins isolated viaVGluRδ2

Category	Protein	gi #	NCBI#	MS 30 mice	MS 50 mice	Sequence coverage (%)	Number of peptides	Score MS (d')	MS/MS 30 mice	MS/MS 50 mice	# peptides	Score MS/MS (d')	Peptide sequences	In control
													NPSQKQPFSSFSR	
	RPTPmam4	13378306	AAK18741	N	N	n/a	n/a	n/a	N	Y	3	n/o	NRSMDVLPLDR DRSSPGALNVYVK DEFQTLNIVTPR	N
	Itpr1	6754390	NP_034715	N	Y	5.6	20	n/o	N	Y	10	n/o	LWSEIPSEIAIDDYDSSGTSKDEIK NKLTFEVVNLAR EAFAIVPVSPAEVR ATVTVNTSDLGNK DQLLEASAATRK DDFILEVDR NLDWFLR NLQEKLESTMK CVVQPEAGDLNNPPK ACNNTSDR	N
	Dnahc8	13310482	AAK18309.1	N	Y	5.9	24	n/o	N	Y	12	0.7	FETLITIHVHQR EELDPALDNVLEK MMRIYVDNAAPDK DWQAFLDLKK KNQYDILDPR IYVDNAAPDK VKNEVQEVK LMEASESVAK IDLQRGTVK LVQLYETSLVR LSLDTMKR DEMDEITQGLISVMKR	N
	Dnahc12	94396852	XP_981204	N	N	n/a	n/a	n/a	N	Y	7	n/o	SIKDVNEPK TDGECVVSAR LVMAAVCVMK SVYCEQGYRIK HGFMLVGEPFAAK LAFDAFLRTAVSGR VFYDRLINDEDR	N
	Zwint	22028168	AAH34870	N	Y	16	5	N/O	N	Y	2	n/o	ATYMDHVDVIK IMEEFMR	N
	Lama1	6678656	NP_032506	N	Y	6.9	16	n/o	N	Y	7	n/o	QHIYAEPFYWR QQGITMKLDELK ASYGQLQQSR LHFMFDLGKGR TLNADLMTLSHR FLKESVGTR TSKSPGPSK	N
	HSP 84	123681	P11499	N	Y	14.7	14	3.8	N	Y	2	n/o	VILHLKEDQTEYLEER GVVDSEDLPLNISR	n/a
	Plekha7	54038521	AAH84587	N	Y	8.6	20	8.4	N	Y	7	n/o	ENYRVLVGSVK RPHTPAER EATIIRHTSVR SRSLLEVPR RAFFFQEK HLSGSSSPPPR	N

Table 3: Proteins isolated viaVGluRδ2

Category	Protein	gi #	NCBI#	MS 30 mice	MS 50 mice	Sequence coverage (%)	Number of peptides	Score MS (d')	MS/MS 30 mice	MS/MS 50 mice	# peptides	Score MS/MS (d')	Peptide sequences	In control
													EQEEERFR	
	Anxa6	13542782	AAH05595.1	Y	Y	45.4	29	13.9	N	Y	2	n/o	DAISGIGTDEK STPEYFAER	N
	4930407I10Rik	94399886	XP_001001646	N	Y				N	Y	5	2.1	KDAVRPSPPNDSSGK CSSAQLASLTSGYGTPGHK SWHNPGGVPEFSIENSR IVRGAGGEEGTETK GGQSSSENDWK	N
	Periphilin 1	94408554	XP_994796	N	N	n/a	n/a	n/a	N	Y	2	1.5	RPPLLDKIPPR YGYGQFQRER	n/a
	Synaptopodin isoform 2	94404501	XP_899657	N	N	n/a	n/a	n/a	N	Y	6	n/o	GAELYAR SSILLIDK AKQAPRPSFSTR RPLGNFTPPPTYAETLSTAPVASRVR SVSPLRSETEARPPSR YTTNAPGGFRVASLSPAR	n/a
	P140	94390735	XP_998750	N	Y	20.6	20	n/o	N	Y	1	n/o	IIAELESGGSSVPPMK	N
Likely Contaminants	Myo18a	28436851	AAH46638.1	Y	Y	20.2	16	n/o	Y	Y	3	n/o	AAQQFSK QGYPDHMVFSEFRR VASGSDLHLTDIDSDSNR	Y
	Myo7b	14161694	NP_115770.1	Y	N	10.3	17	n/o	Y	N	2	n/o	SKLTEEVTK QGLLASENWALGQNDRTGK	n/a
	Spnb2	56206997	CAI25430.1	N	Y	19.7	37	11.5	N	Y	2	n/o	LTTLELLEVR VIESTQDLGNDLAGVMALQR	Y
	Actb	74213524	BAE35572.1	Y	Y	26.6	9	5.9	Y	Y	3	n/o	PRAVFPSIVGR DLTDYLMK TTGIVMDSGDGVTHTVPIYEGYALPHAILR	Y

Proteins isolated via VGluRδ2														
Category	Protein	gi #	NCBI#	MS 30 mice	MS 50 mice	Sequence coverage (%)	Number of peptides	Score MS	MS/MS 30 mice	MS/MS 50 mice	# peptides	Score MS/MS	Peptide sequences	In control
	R-PTP-mu	131570	P28828	N	Y	10.3	14	9^	N	N	n/a	n/a	n/a	N
	Setbp1	51890215	NP_444329.1	Y	N	6.3	11	n/o	Y	N	2	n/o	DIQAFKMNR VPALEPVASFAK	N
	LAMA2	62087424	BAD92159.1	N	Y	6.9	16	n/o	N	Y	1	n/o	LFGEPRAQNEDMEK	n/a
	Mekk3	82800377	XP_890348.1	N	Y	15.1	5	0.3	N	Y	1	n/o	SSPPPGYVPERK	n/a
	Synj1	94400809	XP_978357	N	Y	2.1	3	n/o	N	Y	2	n/o	QLSYNRK SYCRPGPTR	N
	Synj2	37590481	AAH58749	N	Y	8	9	n/o	N	Y	1	n/o	EITHKLSFPSGR	n/a
	Baiap2	13879292	AAH06620.1	Y	Y	34	13	n/o	N	Y	1	n/o	GWFPFSYTR	n/a
	Bai3	28628123	AAO27431.1	Y	N	3.7	9	n/o	Y	N	1	n/o	MMESDYIVMPR	n/a
	LOC70950	30794402	NP_081892.1	N	Y	14.8	16	1	N	Y	1	n/o	TEELEDKLADLK	n/a
	Atp1a1	16307541	AAH10319	N	N	n/a	n/a	n/a	N	Y	2	n/o	TSATWFALSR SPDFTNENPLETR	N
	Atp2a3	31542159	NP_058025	N	Y	8.4	6	n/o	N	Y	1	n/o	MEEAHLLSAADVLR	n/a
	Atp6v1a	31560731	NP_031534	N	Y	11.8	6	n/o	N	Y	1	n/o	AVETTAQSDNK	n/a
	AMPA1	56800448	CAI35291.1	Y	Y	8.9	5	n/o	Y	Y	3	n/o	LNEQGLLDK NGIGYHYILANLGFMDIDLNK IGYWNEDDK	N
	Bai2	110278892	Q8CGM1	N	Y	1.7	3	n/o	N	Y	3	n/o	TCDTGWQRR HQSWSTFK DEYVMLMTWK	n/a
	NEPH1	14572519	AAK00528.1	N	Y	18.8	8	4.8^	N	Y	2	n/o	FSQEPADQTVVAGQR DGLALGMGQGLK	N
	Ant1	902008	AAC52837	N	Y	31.8	10	2.9	N	n/a	n/a	n/a	n/a	n/a
	4833417A11Rik	94363638	XP_992319	N	N	n/a	n/a	n/a	N	Y	4	n/o	EKPNDPTLELISETLK GNHTKDFLTYK KDQKPMER NVFPGTYGMAAPWYFPILPSYWK	N
	LOC672116	94369146	XP_996336	N	N	n/a	n/a	n/a	N	Y	3	1.1	RIHTEEKPYK ILQEAQKNVR GLTFANQSSYIKVHK	Y
	Ranbp2	10442646	AAG17403.1	N	Y				N	Y	1	n/o	FGIWGWEDCTSVR	N
	Ncoa7	50369666	AAH76623	N	Y	5	3	n/o	N	Y	2	n/o	FNVTAEGDHSTDDKK SFASHTATMVQQYSKR	n/a
	Grik4	109730793	AAI18011	N	Y				N	Y	1	n/o	LCGAGEPDQLAQR	n/a
	Gabbr2	94373276	XP_980699	N	Y				N	Y	1	n/o	HRHVPPSFR	n/a
	Synaptopodin	48428644	Q8CC35	N	Y	10.2	10	n/o	N	Y	1	n/o	HPSPQSPSR	n/a
	Nesprin 2	82942816	XP_619002.2	Y	N	14.6	22	n/o	Y	N	2	n/o	IQDQPPGNSSGTSLSK AQLDDALPSPLK	n/a
	GluR3	84781717	NP_058582	Y	Y	13.8	14	4.4	N	N	3	n/o	SAEPSVFTK IWNGMVGELVYGR DIQEFR	n/a
	Plb1	94376138	XP_997033	N	N	n/a	n/a	n/a	N	Y	1	n/o	KFNPSITGFSTGTLDNK	n/a
	Fondrin alpha chain	82799702	XP_929370	N	Y	16	25	3.3	N	n/a	n/a	n/a	n/a	n/a
	mKIAA4061	60360496	BAD90492	N	N	n/a	n/a	n/a	N	Y	4	1.2		n/a

SUPPORTING INFORMATION for Selimi et al. 2009

Supplementary methods

1. Antibodies

The following antibodies were used (dilution): Rabbit anti-GluRδ2, Chemicon # AB1514 (1/2000); Mouse anti-GluR2, Chemicon #MAB397 (1/500); Mouse anti-PSD95, Affinity Bioreagents #MA1-046 (1/2000); Rabbit anti-PSD93 Chemicon #AB5168 (1/100); Mouse anti-NR2A, Chemicon #MAB5216 (1/500); Mouse anti-Gephyrin, BD transduction Laboratories #610584 (1/250); Mouse anti-GABA(A) receptor β2/3, Upstate #05-474 (1/1000); Rabbit anti- GABA(A) receptor α1, Upstate #06-868 (1/1000); Rabbit anti- GABA(A) receptor α6, Chemicon #AB5610 (1/2500); Rabbit anti-Homer (H-342), Santa Cruz #sc-15321 (1/200); Mouse anti-BiP/GRP78, BD transduction Laboratories #610978 (1/500); Mouse anti-COX (cytochrome oxidase subunit I), Molecular Probes #A6403 (1/20000); Rabbit anti-RPTPmu, Abcam #ab23820; Goat anti-BAIAP2, Abcam #ab15697; Rabbit anti-delta2 Catenin, Abcam # ab11352; Rabbit anti-mGluR1, Abcam #ab6439 (1/1000); Guinea pig anti-VgluT1, Chemicon (1/3000); Guinea pig anti-VgluT2, Chemicon (1/3000); Mouse anti-GAD65/67, Stressgen bioreagents #MSA-225 (1/500); Rabbit anti-synapsin I #AB1543, Chemicon (1/1000); Mouse anti-synaptophysin #611880, BD Biosciences (1/5000).

Rabbit anti-Neph1 was a generous gift from Pr. Sumant Chugh.

The polyclonal anti-Gm941 antibody was custom-generated by injection into rabbits of peptide #1, LKEGDEEIKSDIYTLC, and peptide#2, PLKVERAPAPHGPC. Bleeds were purified using protein G and then affinity-purified against peptide # 2 (Green Mountain Antibodies, Burlington, USA).

The polyclonal anti-MRCK gamma antibody was custom-generated by injection into rabbits of the following peptide: SERPRSLPPDPESESSPC. Bleeds were purified using protein G and then affinity-purified against the peptide (Green Mountain Antibodies, Burlington, USA).

The anti-GFP antiserum was generated by injection in a goat of the full-length GFP (Green Mountain Antibodies) and was affinity-purified using a column made of Sepharose-4B resin coupled to full-length GFP.

2. BAC modification and transgenic mice

The cDNA encoding GluRδ2 together with the 3'UTR was amplified from cerebellar RNA, and placed in frame with a preprotrypsin signal sequence and Venus in a building vector based on eGFP-C2 (Clontech, Mountain View, USA). The sequence encoding the tagged VGluRδ2 and the SV40 polyadenylation signal from the building vector were subcloned into the PL53.SC-AB shuttle vector. The Pcp2 containing BAC RP23-192G13 was then modified by homologous recombination using this shuttle vector and the two-step method (Gong S. et al., 2002, *Genome Res*, **12**:1992). Recombination boxes of 1 kb were amplified from the BAC genomic DNA using the following primers: for box A, 5'TTGGCGCGCCGGTTCCACCCTCATGTTG3' and 5'AGCTTTGTTTAAACCCGATCGCCCTGCACGTGGGG3'; for box B, 5' ATAAGAATGCGGCCGCCGGCTTTCTGGGTTCTGGC3' and 5'ATAAGAATGCGGCCGCGTTTAAGCCAGGTGTGGG3'. These recombination boxes allow the replacement of the Pcp2 ATG by the cDNA construct. Correct modification of the Pcp2 BAC was visualized by southern blot on BAC DNA digested by EcoRI, separated on 0.8% agarose gel and probed with P^{32}dATP labeled box A. Pulse field gel electrophoresis was performed on BAC DNA digested by SpeI.

A correctly modified BAC was purified by cesium chloride and DNA was then dialyzed in oocyte injection buffer for generation of transgenic mice. Integration of the BAC in the mouse genome was visualized by southern blot using genomic DNA digested by EcoRI and box A as a probe.

3. Protein extracts for expression analysis

Total protein extracts from cerebellum were prepared by homogenizing the tissue and incubating for 30 minutes at 4°C in a buffer containing 50 mM Tris-Cl, 150mM NaCl, 0.1% SDS, 0.5% sodium deoxycholate and 1% NP-40 complemented with a protease inhibitor cocktail. The homogenate was then sonicated and centrifuged 30 minutes at maximum speed to provide the supernatant for western blot analysis.

For immunoprecipitation experiments, the homogenate from each cerebellum was incubated in 50 mM Tris-Cl, pH=7.4, containing 1% Triton X-100 final for 30 minutes and then centrifuged at maximum speed. The supernatant was affinity-purified using 0.5 mg anti-GFP coated dynabeads for one hour at 4°C. Beads were washed with 50 mM Tris-Cl, pH=7.4, containing 1% Triton X-100 and immunocomplexes eluted for western blot analysis.

4. Western blot

Protein samples (dissolved in NuPAGE LDS sample buffer, Invitrogen, Carlsbad, USA) were separated on 4-12% NuPAGE Bis-Tris gels (Invitrogen). Proteins were then transferred using the semi-dry method (SD transfer cell, Biorad, Hercules, USA) on Immobilon-P PVDF membrane (Millipore, Bedford, USA). Antibodies were diluted in

5% milk/PBS/0.2% tween-20. Secondary antibodies were conjugated to horseradish peroxidase (Pierce) and detection performed using a chemoluminescent substrate.

5. Immunofluorescence

Mice were perfused transcardiacally using 4% paraformaldehyde in phosphate buffer saline pH=7.4 (PBS), then 10% sucrose in PBS. Brains were incubated for 3 days in 30% sucrose in PBS. 25 μm-thick cerebellar sections were cut using a freezing sliding microtome.

For detection of VGluRδ2, sections were incubated in 0.3% H_2O_2 in PBS at 4°C, washed in PBS and preincubated in 4% normal donkey serum in PBS. Incubation with the goat anti-GFP antibody (diluted 1/25000 in 1% normal donkey serum/PBS/1%TritonX100/0.1%fish gelatin) was performed overnight at 4°C. Immunolabeling was detected using a biotinylated anti-goat secondary antibody (1/5000 in PBS/1%TritonX100/0.1% fish gelatin) followed by amplification using streptavidin-HRP (1/500) and TSA-FITC (Perkin Elmer, Waltham, USA). All washes were performed in PBS/1%TritonX100.

For detection of the other antigens by immunofluorescence, sections were incubated overnight with the corresponding antibodies and mouse anti-calbindin (1/5000, Swant, Bellinzona, Switzerland) diluted in 1% normal donkey serum/PBS/0.2%TritonX100. Immunolabeling was detected using an Alexa-488 conjugated anti-rabbit or anti-goat and a Rhodamine-RedX conjugated anti-mouse or Cy3 conjugated anti-guinea pig. All washes were performed in PBS/0.2% Triton X-100.

Pictures were taken using a LSM 510 laser scanning confocal microscope (Carl Zeiss, Thornwood, USA).

6. Database searching using MS and MS/MS mass spectrometric data:

We used the XProteo computer algorithm (www.xproteo.com) search the NCBI database with MS and MS/MS data. The parameters used for searching the MS data were: Data type: MS; Species: Mus musculus (although for detecting the tag, searches in All entries were performed); NCBI database; protein mass 0-300 kDa; protein pI: 1-14; Mixture Search: Auto; Display top: 20; Enzyme: Trypsin; Max. missed cleavages: 1; Mass type: Monoisotopic; Charge state: MH+; Mass tolerance: 0.03 Da.

Due to the low quantities of sample, the MS/MS CID data was acquired and interpreted manually. This helped limit the number of acquired microscans to that optimal for each peptide fragmentation and it reduced the redundancy in confirming the presence of the more abundant proteins. After manual interpretation, the MS/MS CID data was converted to dta files and also searched in the database using XProteo. The parameters used for searching the MS/MS data were: Data type: MS/MS; Species: Mus musculus; NCBI database; protein mass 0-300 kDa; protein pI: 1-14; Mixture Search: Auto; Display top: 20; Enzyme: Trypsin; Max. missed cleavage: 1; Mass type: Monoisotopic; Charge state: MH+; Precursor tolerance: 0.03Da; Fragment tolerance: 0.6Da; Instrument: MALDI_I_TRAP. Any new assignment made by XProteo was carefully checked manually.

The candidate proteins were scored by XProteo using probability scores calculated with an improved version of the ProFound Bayesian algorithm (Zhang, W. and Chait, B.T., ProFound: an expert system for protein identification using mass spectrometric peptide mapping information. *Anal. Chem.* **72**, 2482-2489 (2000)). The XProteo algorithm then measures the d' (discriminability) for each candidate protein as the normalized distance between the score distribution (of the candidate protein) and the distribution of randomly matched proteins (in units of standard deviation). A score of d'=4 correspond to a true positive rate of 0.99 and a false positive rate of 0.05.

From our experience, the identities of proteins with d' > 4 could virtually always be readily confirmed by MS/MS. However, we note that low molecular weight proteins and proteins present as complex mixtures often yielded d' < 4. We tested many of these putative lower confidence identifications by MS/MS, which often allowed for their subsequent confirmation.

7. MS/MS hypothesis-driven approach:

To confirm the specificity of the isolated proteins, immunoaffinity purifications were also performed on preparations from Pcp2/eGFP transgenic mice (GFP). The sample preparation was identical to that performed for the isolations of VGluRδ2 from Pcp2/VGluRδ2 mice as described in the material and methods section of the manuscript. The analysis of the proteins isolated in the control experiment were performed using MALDI QqToF MS and MALDI IT MS/MS analysis as described for the isolations of VGluRδ2. However, even if a protein was not observed in the control samples using these analyses, we performed additional experiments to probe for their presence at lower levels and the specificity of the observed associations. The approach we utilize is termed hypothesis-driven multistage mass spectrometry and previously described (Kalkum M et al, PNAS 2003 Mar 4;100(5):2795-800). Briefly, we searched in the corresponding control samples for the presence of peptides that we confirmed to correspond to proteins isolated with VGluRδ2. Even if peptides were not observed in the control samples at the MS level, their corresponding *m/z* value ($[M+H]^+$) was selected and subjected for CID fragmentation and analyzed using MALDI IT MS/MS analyses. This strategy allows the highly sensitive detection of specific peptides from specific proteins, even if the peptide species cannot be discerned in the primary MALDI-ToF analysis because of insufficient signal-to-noise.

Supplementary references

1. www.brain-map.org

2. www.stjudebgem.org.

3. Yuzaki, M., The delta2 glutamate receptor: 10 years later. Neurosci Res, 2003. 46(1): p. 11-22.

4. Uemura, T., H. Mori, and M. Mishina, Direct interaction of GluRdelta2 with Shank scaffold proteins in cerebellar Purkinje cells. Mol Cell Neurosci, 2004. 26(2): p. 330-41.

5. Shiraishi, Y., et al., Differential expression of Homer family proteins in the developing mouse brain. J Comp Neurol, 2004. 473(4): p. 582-99.

6. Fukaya, M. and M. Watanabe, Improved immunohistochemical detection of postsynaptically located PSD-95/SAP90 protein family by protease section pretreatment: a study in the adult mouse brain. J Comp Neurol, 2000. 426(4): p. 572-86.

7. Roche, K.W., et al., Postsynaptic density-93 interacts with the delta2 glutamate receptor subunit at parallel fiber synapses. J Neurosci, 1999. 19(10): p. 3926-34.

8. Miyagi, Y., et al., Delphilin: a novel PDZ and formin homology domain-containing protein that synaptically colocalizes and interacts with glutamate receptor delta 2 subunit. J Neurosci, 2002. 22(3): p. 803-14.

9. Lambolez, B., et al., AMPA receptor subunits expressed by single Purkinje cells. Neuron, 1992. 9(2): p. 247-58.

10. Lujan, R. and R. Shigemoto, Localization of metabotropic GABA receptor subunits GABAB1 and GABAB2 relative to synaptic sites in the rat developing cerebellum. Eur J Neurosci, 2006. 23(6): p. 1479-90.

11. Moga, M.M. and D. Zhou, Annexin 6 immunoreactivity in select cell populations in the rat brain. J Histochem Cytochem, 2002. 50(9): p. 1277-80.

12. Ichikawa, T., et al., Ca2+/calmodulin-dependent protein kinase II in the rat cerebellum: an immunohistochemical study with monoclonal antibodies specific to either alpha or beta subunit. J Chem Neuroanat, 1992. 5(5): p. 383-90.

13. Ching, G.Y., et al., Overexpression of alpha-internexin causes abnormal neurofilamentous accumulations and motor coordination deficits in transgenic mice. J Neurosci, 1999. 19(8): p. 2974-86.

14. Baba-Aissa, F., et al., Purkinje neurons express the SERCA3 isoform of the organellar type Ca(2+)-transport ATPase. Brain Res Mol Brain Res, 1996. 41(1-2): p. 169-74.

15. Kudo, M., et al., Localization of mRNAs for synaptojanin isoforms in the brain of developing and mature rats. Brain Res Mol Brain Res, 1999. 64(2): p. 179-85.